Cell Metabolism

Article

FGF21 promotes longevity in diet-induced obesity through metabolic benefits independent of growth suppression

Graphical abstract

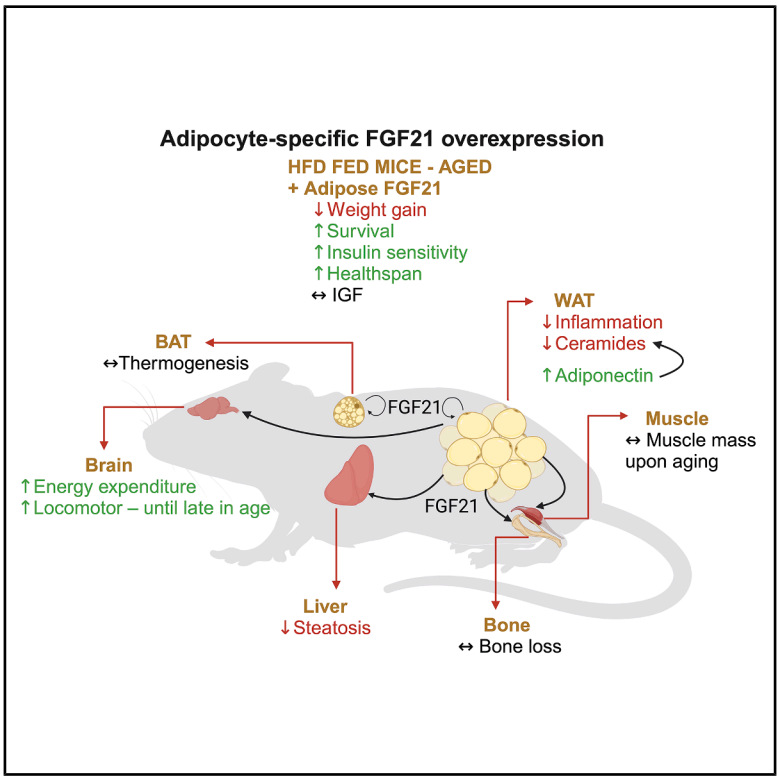

Highlights

- FGF21 overexpression in the adult mouse increases survival that is not linked to trade-offs in organismal growth
- FGF21 overexpression prevents obesity, liver steatosis, and loss of lean mass in gerobese mice fed a HFD
- Elevated FGF21 increases energy expenditure but does not affect cold tolerance in mice fed a HFD
- FGF21 reduces ceramide levels in visceral adipose tissue by adiponectin-independent mechanisms

Authors

Christy M. Gliniak, Ruth Gordillo, Yun-Hee Youm, ..., Tamas L. Horvath, Vishwa Deep Dixit, Philipp E. Scherer

Correspondence

philipp.scherer@utsouthwestern.edu

In brief

This study demonstrates that inducible, adipocyte-specific overexpression of FGF21 in adult male mice improves metabolic health and extends lifespan during high-fat diet feeding. These benefits occur independently of growth suppression and are associated with reduced visceral adipose inflammation and ceramide levels, offering mechanistic insights into FGF21's pro-longevity effects under metabolic stress.

Gliniak et al., 2025, Cell Metabolism *37*, 1547–1567
July 1, 2025
https://doi.org/10.1016/j.cmet.2025.05.011

CellPress

Cell Metabolism

CellPress

Article

FGF21 promotes longevity in diet-induced obesity through metabolic benefits independent of growth suppression

Christy M. Gliniak,[1] Ruth Gordillo,[1] Yun-Hee Youm,[2] Qian Lin,[1] Clair Crewe,[1,3] Zhuzhen Zhang,[1,4] Bianca C. Field,[1] Teppei Fujikawa,[5,6] Megan Virostek,[1] Shangang Zhao,[1,7] Yi Zhu,[1,8] Clifford J. Rosen,[9] Tamas L. Horvath,[10,11] Vishwa Deep Dixit,[2] and Philipp E. Scherer[1,12,*]

[1]Touchstone Diabetes Center, University of Texas Southwestern Medical Center, Dallas, TX, USA
[2]Department of Pathology, Immunobiology and Comparative Medicine, Yale Center for Research on Aging (Y-Age), Yale School of Medicine, New Haven, CT, USA
[3]Department of Cell Biology and Physiology and the Department of Internal Medicine, Division of Endocrinology, Metabolism and Lipid Research, Washington University School of Medicine, St. Louis, MO, USA
[4]College of Life Sciences, Wuhan University, Wuhan, China
[5]Center for Hypothalamic Research, Department of Internal Medicine and the Peter O'Donnell Jr. Brain Institute, University of Texas Southwestern Medical Center, Dallas, TX, USA
[6]Institute of Human Life and Ecology, Osaka Metropolitan University, Osaka, Japan
[7]Sam and Ann Barshop Institute for Longevity and Aging Studies, Division of Endocrinology, Department of Medicine, University of Texas Health Science Center at San Antonio, San Antonio, TX 78229, USA
[8]Department of Pediatrics, Baylor College of Medicine, Houston, TX, USA
[9]Center for Molecular Medicine, MaineHealth Institute for Research, Scarborough, ME, USA
[10]Department of Comparative Medicine, Yale School of Medicine, New Haven, CT, USA
[11]Department of Anatomy and Histology, University of Veterinary Medicine, Budapest 1078, Hungary
[12]Lead contact
*Correspondence: philipp.scherer@utsouthwestern.edu
https://doi.org/10.1016/j.cmet.2025.05.011

SUMMARY

Approximately 35% of US adults over 65 are obese, highlighting the need for therapies targeting age-related metabolic issues. Fibroblast growth factor 21 (FGF21), a hormone mainly produced by the liver, improves metabolism and extends lifespan. To explore its effects without developmental confounders, we generated mice with adipocyte-specific FGF21 overexpression beginning in adulthood. When fed a high-fat diet, these mice lived up to 3.3 years, resisted weight gain, improved insulin sensitivity, and showed reduced liver steatosis. Aged transgenic mice also displayed lower levels of inflammatory immune cells and lipotoxic ceramides in visceral adipose tissue, benefits that occurred even in the absence of adiponectin, a hormone known to regulate ceramide breakdown. These results suggest that fat tissue is a central site for FGF21's beneficial effects and point to its potential for treating metabolic syndrome and age-related diseases by promoting a healthier metabolic profile under dietary stress and extending healthspan and lifespan.

INTRODUCTION

Improving healthspan, the period of life spent in good health, is crucial for enhancing the quality of life and potentially extending the lifespan of an aging population. Currently, 35%–40% of adults aged 65 and above are classified as obese, a condition that, combined with aging, independently increases the risk of chronic diseases.[1,2] Understanding how the interplay between obesity and aging affects healthspan and lifespan is essential for developing effective therapeutic strategies.

Fibroblast growth factor 21 (FGF21) is an atypical member of the FGF family, functioning as an endocrine hormone primarily secreted by hepatocytes into circulation in response to various cellular stressors.[3,4] FGF21 has garnered significant interest as a therapeutic agent due to its promising effects in treating metabolic conditions in mice and humans, including type 2 diabetes and non-alcoholic fatty liver disease.[5–8] Despite these well-documented benefits, the precise mechanisms through which FGF21 exerts its effects on multiple organs remain incompletely understood.

In addition to the liver, FGF21 is produced locally in thymic epithelial cells,[9] adipocytes,[10] muscle,[11] and the pancreas,[12] which may exert significant autocrine and paracrine effects.[4] FGF21 signals through a heteromeric receptor complex composed of FGF receptor 1c (FGFR1c) and the co-receptor β-Klotho.[13,14] While FGFR1c is widely expressed across various

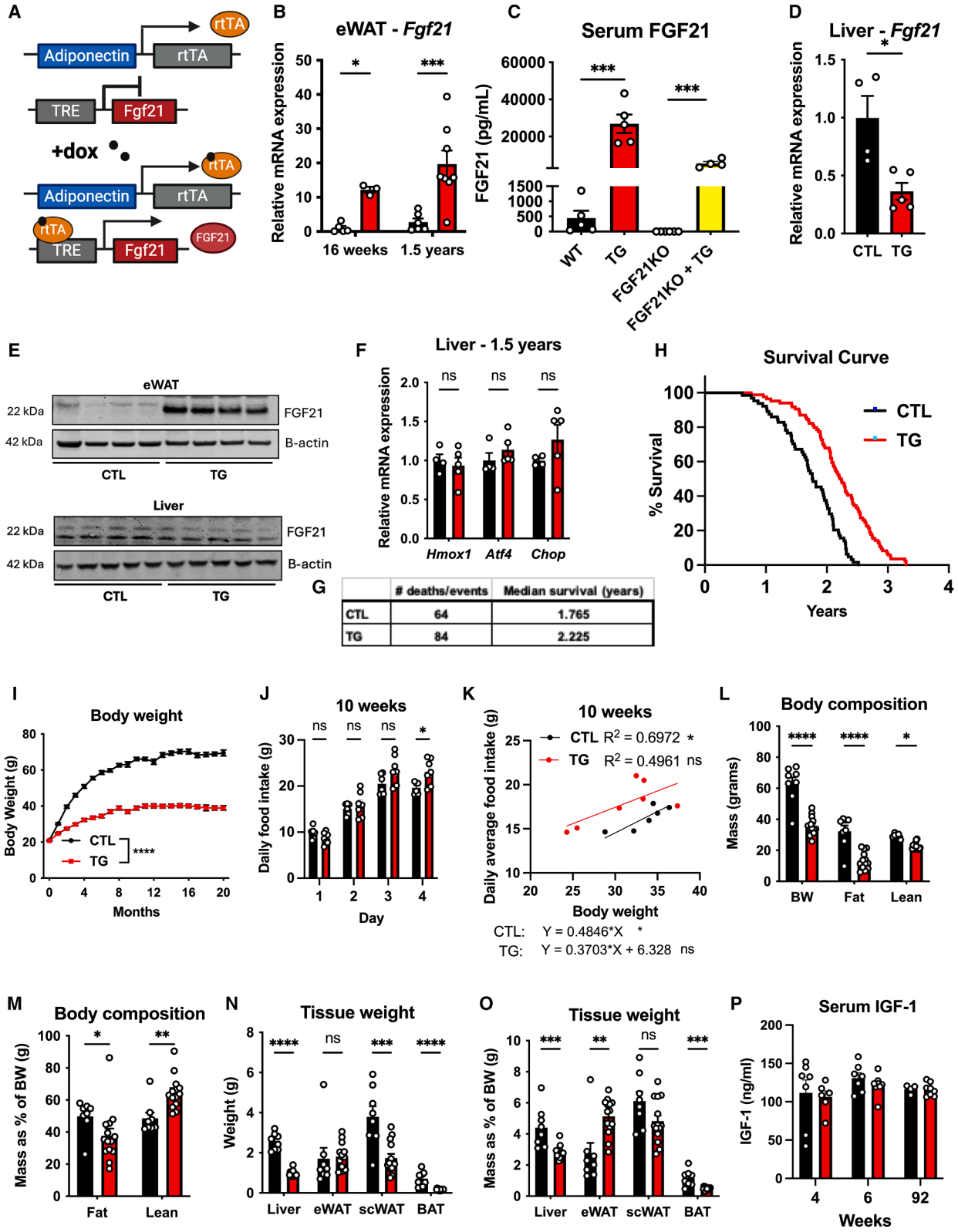

Figure 1. Adipocyte-specific FGF21 overexpression enters circulation and extends lifespan

(A) Scheme illustrating doxycycline-inducible, adipocyte-specific FGF21 overexpression in mice.

(B) *Fgf21* mRNA levels in eWAT from male control and TG mice fed HFD+dox for 16 weeks or 1.5 years beginning at 10–12 weeks of age (n = 3–8).

(legend continued on next page)

tissues, β-Klotho expression is restricted mainly to the brain, liver, and adipose tissue, indicating these as primary targets for FGF21 action.[4,15] Receptor studies performed in mice suggest that FGF21's endocrine actions in the central nervous system (CNS) and adipose tissue are crucial in enhancing energy expenditure and improving insulin sensitivity.[16] While the local effects of FGF21 in adipose and other tissues are recognized as being highly significant, research in this area remains limited.

The literature overwhelmingly supports FGF21's benefits on aging-related pathways, and thus, FGF21 is coined as a pro-longevity hormone. However, few studies directly investigate the effect of FGF21 on longevity. Zhang et al. show that constitutive expression of FGF21 from the liver can significantly extend lifespan in mice. This effect was attributed to increased energy expenditure and modulation of growth pathways, including insulin-like growth factor (IGF) and growth hormone (GH) signaling.[17,18] However, these findings stem from constitutive early expression of FGF21 in mice, which results in developmental abnormalities and dwarfism.[18,19] Thus, it is critical to reassess FGF21's effect in normal mice and under conditions more relevant to human disease and aging.

There is supporting evidence that FGF21 plays a pivotal role in mediating various aspects of the adaptive starvation response, a process associated with enhanced longevity.[20] Hill et al. showed that the deletion of FGF21 reverses the beneficial effects of dietary protein restriction to increase lifespan.[17] However, since metabolic aging in most of the world population is related to overnutrition, additional studies should address FGF21's role in obesity.

There is a knowledge gap for the precise mechanisms through which FGF21 extends lifespan in adult organisms, particularly within the framework of obesity. To address this, we developed a mouse model with inducible, adipocyte-specific overexpression of FGF21, enabling an investigation into whether localized elevation of FGF21 can influence systemic metabolic outcomes and longevity under the metabolic stress of high-fat diet (HFD) feeding. Importantly, the inducible nature of this model allows for the targeted expression of FGF21 in adult mice, thereby avoiding congenital effects that could obscure the mechanism of action of the hormone.

In this study, we demonstrate that adipocyte-specific overexpression of FGF21 not only mitigates the metabolic detriments of a HFD but also significantly extends median survival in transgenic mice compared with control mice (2.225 vs. 1.765 years). Individual mice with adipocyte-specific overexpression of FGF21 lived up to 3.3 years of age. Throughout the lifetime of these mice, FGF21 overexpression led to improvements in serum lipid profiles, enhanced glucose tolerance, and increased insulin sensitivity. These metabolic benefits were independent of growth defects and energy expenditure in aged mice. Notably, FGF21 profoundly affected visceral adipose tissue, the fat depot most closely associated with metabolic pathology, by reducing inflammatory immune cell populations and the accumulation of inflammatory sphingolipids known as ceramides. This ceramide-lowering effect was maintained even in the absence of adiponectin, a known mediator of FGF21 and ceramide levels.

In summary, our findings demonstrate that elevated FGF21 in adult mice promotes healthspan and extends lifespan, not by altering growth, but by fostering healthy adipose tissue and lowering ceramide levels—each contributing to preserving organ function during aging. These results suggest that the GH axis, energy expenditure, and browning of subcutaneous fat may be part of FGF21's lifespan-extending mechanisms in lean mice but not during overnutrition. Additionally, our results show that visceral adipose tissue is one of the main targets mediating the systemic benefits of FGF21, offering new insights into potential therapeutic strategies to combat the metabolic and inflammatory consequences of aging and obesity.

RESULTS

Mouse model of adipocyte-specific FGF21 overexpression

To investigate the impact of FGF21 expression on lifespan restricted to adult mice, we generated an inducible mouse model of FGF21 overexpression specific to adipocytes. This genetic model limits *Fgf21* mRNA expression to epididymial white adipose tissue (eWAT), subcutaneous white adipose tissue (scWAT), and brown adipose tissue (BAT) in transgenic mice fed dietary doxycycline (dox; Figures 1A–1E and S1A–S1D). FGF21 mRNA and protein decreased in the liver in transgenic (TG) mice compared with control mice (Figures 1D and 1E). The resulting transgenic adipocyte-specific overexpression model is herein referred to as the TG mouse, and mice with the adiponectin-rtTA allele are the controls. These studies were performed in male mice on the C57Bl/6 background, and both TG and controls were fed doxycycline at the indicated time points. Basal circulating levels of FGF21 are low. Nutrient or cellular stress induces its expression to high levels, and it is quickly cleared from circulation.[21,22] This elevation of serum FGF21 observed in TG mice represents a physiological level

(C) Serum FGF21 levels from control mice and FGF21 whole-body knockout mice with or without adipose-tissue-specific FGF21 overexpression (n = 4–6).
(D–F) Control and TG mice were fed HFD-dox for 1.5 years. *Fgf21* mRNA levels in the liver (n = 4–5) (D) Western blot for FGF21 and β-actin protein expression in eWAT and liver (E) (n = 4). mRNA levels for stress-associated genes in the liver (F) (n = 3–5).
(G and H) Median survival (G) and Kaplan-Meyer survival curves (H) for control and TG mice fed HFD-dox (n = 64–84).
(I) Body weight in male control and TG mice was fed HFD+dox. (n = 59–81).
(J) Daily food intake was measured when HFD was initiated at 10 weeks of age (n = 6–7).
(K) Linear regression for food intake calculated with body mass as a covariate (J) (n = 6–7).
(L–O) Male control and TG mice were fed HFD+dox for 1.5 years. Body composition (L) (n = 8–14) and body composition calculated as percent of body weight (M) (n = 8–14). Tissue weights (N) (n = 8–14) and tissue weights calculated as percent of body weight (O) (n = 8–14).
(P) Free IGF levels in control and TG mice fed a HFD+dox for 4, 6, or 92 weeks (n = 4–8).
Error bars represent mean ± SEM. n number for (A)–(P) denotes biological replicates. p values were determined by log-rank (Mantel-Cox) test (G–I). Significance for (I) was calculated by two-way ANOVA and significance between control and TG mice. Significance for (B)–(D), (F), (I), (J), and (L)–(P) was calculated using a two-tailed Student's t test. Determination of the coefficient of determination (R-squared) for (K) was determined by linear regression analysis. ns, $p > 0.05$, $^{*}p < 0.05$, $^{**}p < 0.01$, $^{***}p < 0.001$, and $^{****}p < 0.0001$.

equivalent to about five times higher than levels induced by fasting conditions, similar to other models of FGF21 overexpression (Figures S1E–S1G).[19] Investigating mice with elevated and continued FGF21 overexpression is relevant in the context of long-acting FGF21 agonists that are effective in clinical studies.

To identify the principal source of FGF21 in our mouse model, we bred FGF21 whole-body knockout mice with mice overexpressing FGF21 in the adipose tissue.[23] There is no expression of FGF21 in the FGF21 whole-body knockout mice, and serum FGF21 levels significantly rose upon overexpressing FGF21 in the adipose tissue (Figure 1C). Major drivers of FGF21 secretion in the liver, such as amino acid deprivation or markers of endoplasmic reticulum (ER) stress (*Hmox1*, *Atf4*, and *Chop*), did not differ between TG and control mice (Figure 1F). Not only does this study design prevent dwarfism in mice, but it also avoids the stress of a low-protein diet that would trigger FGF21 expression from the liver (Figure S1H). These data indicate a mouse model where FGF21 expression is increased through local FGF21 production in adipose tissue, which contributes to elevated circulating FGF21 and does not involve a contribution by the liver. Many genetic and pharmacological studies in mice investigated FGF21 mechanisms in the short term. However, this is the first mouse model to be exposed to FGF21 throughout aging. Thus, any potential phenotype observed in TG mice may be attributed to increased adipose tissue-derived FGF21 in circulation.

FGF21 overexpression in the adult mouse increases the survival of mice fed a HFD

Congenital, transgenic overexpression of FGF21 that inhibits the somatotropic axis markedly extends lifespan in mice fed a chow diet.[19] Therefore, we investigated whether inducible FGF21 overexpression in adult mice (10–12 weeks of age) would increase longevity during HFD feeding. Adipocyte-specific FGF21 expression significantly increased median survival compared with control mice (2.225 vs. 1.765 years) (Figure 1G). Remarkably, higher circulating FGF21 increased lifespan to an exceptional degree for mice fed HFD-dox, with several living up to 3.30 years of age (Figure 1H). For context, the TG mice fed HFD-dox in this study achieved a median survival similar to that of normal chow-fed male mice in previous studies (2.32 years).[19] These data indicate that increasing adipocyte FGF21 expression during adulthood effectively mitigates the effects of aging, resulting in increased lifespan.

FGF21 overexpression prevents obesity and loss of lean mass in aged mice

Obesity and dysfunctional adipose tissue are major contributors to the systemic derangements in glucose and lipid metabolism that lead to aging-associated disease. Mice with adipocyte-specific FGF21 overexpression gained less body weight (BW) on HFD-dox and remained lean throughout advanced age compared with control mice (Figure S1I). Furthermore, inducing FGF21 expression in obese mice caused significant weight loss that was maintained through advanced age (Figure S1J). Daily food intake was assessed in 10-week-old mice upon initiating HFD-dox and throughout their lifespan at 10 and 18 months of HFD-dox feeding. At the initiation of HFD at 10 weeks of age, TG mice gained less body weight than the control mice (Figure 1). Calculation of *R*-squared values and representation of the data as regression between food intake and body mass show that food intake in transgenic mice at 10 weeks of age and 10 and 18 months of HFD feeding was not dependent on body weight (Figures 1J, 1K, S1K, S1L, S2A, and S2B). By contrast, control mice at 10 weeks of age and 18 months of HFD feeding displayed a significant positive association between food intake and body weight, but not at 10 months (Figures 1J, 1K, S1K, S1L, S2A, and S2B). The increased food intake data in control mice is consistent with the weight gain observed over their lifespan. TG mice maintained a lower body weight, and there was no evidence of lowered food intake compared with controls. Considered a "starvation hormone," FGF21 coordinates adaptive changes in food intake preferences and drives increased protein intake in mice.[24,25] Our results are consistent with studies showing that FGF21-mediated weight loss during adequate protein intake is primarily due to increased energy expenditure.[26] This indicates that the weight-lowering action of FGF21 in these prior and current studies is independent of calorie restriction.

Body composition assessments determined that FGF21 led to decreased fat and lean mass as early as 16 weeks and up to 1.5 years of HFD compared with control mice (Figures 1L and S2C–S2G). When tissue masses were normalized to body weight, the fat mass decreased, and lean mass increased in TG mice compared with controls (Figures 1M, S2F, and S2G)—at 6 months and 1.5 years of HFD-dox, tissue masses for liver, scWAT, and BAT decreased, with no change in eWAT comparing TG mice to control mice (Figures 1N and S2H). Interestingly, the proportion of eWAT increased in TG mice vs. control mice (Figure 1O). Together, these findings demonstrate that increasing adipose tissue FGF21 can have significant benefits in preventing obesity, decreasing fat mass, and preserving lean mass.

FGF21's pro-longevity responses are not linked to trade-offs in organismal growth

One mechanism attributed to the anti-aging effects of FGF21 involves the reduction of GH and insulin-like growth factor-1 (IGF-1) signaling that regulates development and cellular growth. However, whether this exact mechanism operates when FGF21 is induced in adult mice or the circumstances of HFD feeding remain unclear. Upon adipocyte-specific FGF21 overexpression, free IGF-1 levels did not differ from control mice, irrespective of age (Figure 1P). Moreover, lean mass increased in TG mice in proportion to BW compared with control mice, indicating a lack of muscle catabolism (Figures 1L and 1M). We then evaluated additional measures of FGF21's impact on development. FGF21 has a strong pathophysiological connection to bone homeostasis regulation and development.[27–29] After 1.7 years on a HFD, there were no significant differences in tibia length, trabecular bone mineral density, or cortical tissue mineral density between TG and control mice despite the former's lower body weight (Figures 2A, 2B, S2I, and S2J). Serum indicators of metabolic dysfunction, such as blood urea nitrogen (BUN), lactate, sodium, and magnesium, did not differ significantly between the groups (Figures S2K–S2N). These findings suggest that lifespan extension due to FGF21 overexpression is not primarily driven by reduced growth or development or energy expenditure but instead attributed to the paracrine and endocrine actions of FGF21 in peripheral organs.

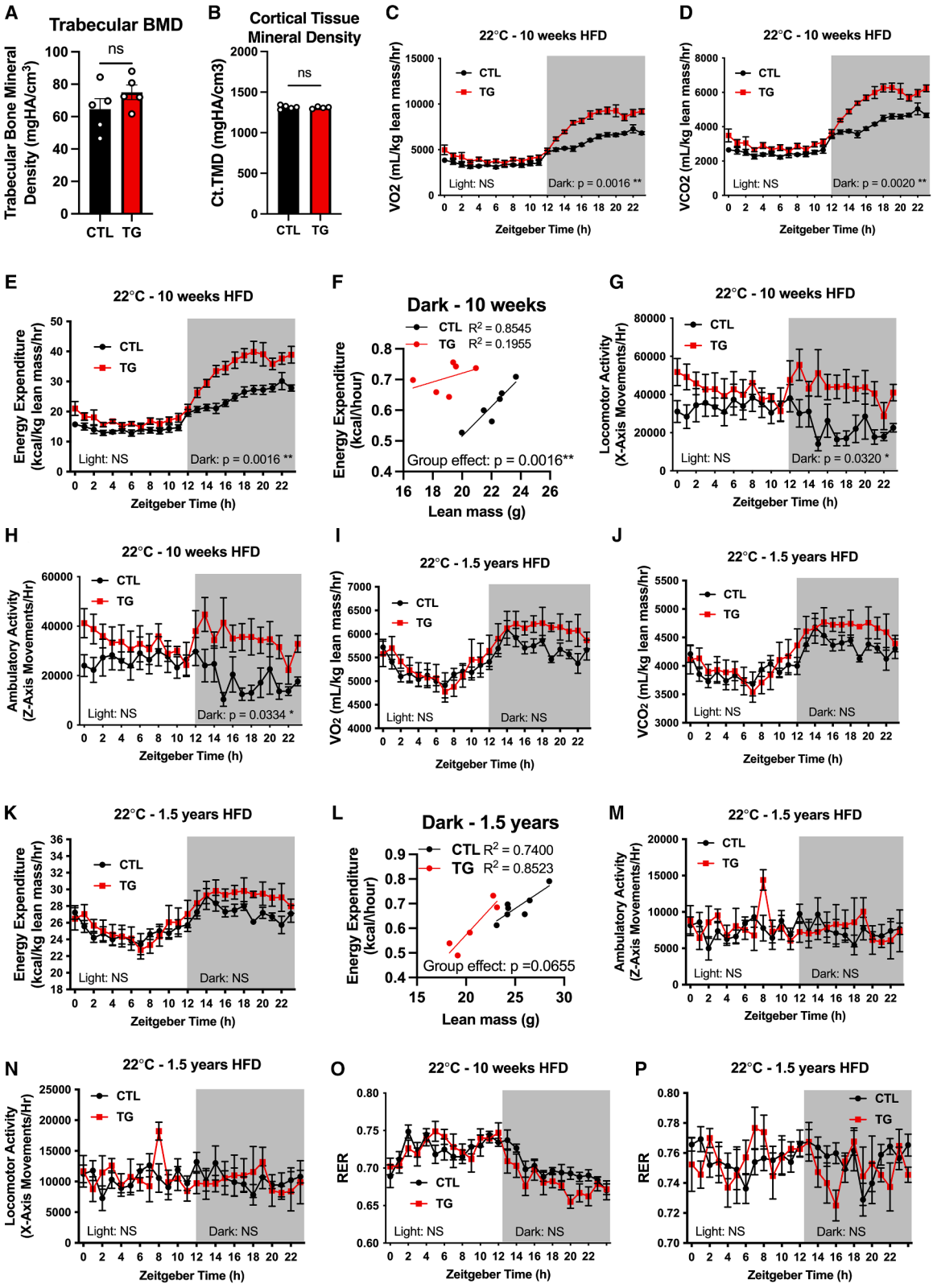

Figure 2. Overexpression of FGF21 in adipocytes increases energy expenditure and improves body composition in response to HFD

(A and B) Male control and TG mice were fed HFD+dox for 1.7 years beginning at 10–12 weeks of age. Trabecular bone density (A) (n = 5) and cortical tissue mineral density (B) (n = 4–5).

(legend continued on next page)

FGF21 increases energy expenditure in young mice fed a HFD

Adipocyte-specific FGF21 overexpression promoted weight loss despite increased food intake. Therefore, we assessed whether there were changes in energy expenditure. Indirect calorimetry was performed after 10 weeks or 1.5 years of HFD-dox, and the analyses were normalized by lean mass (Tables S1 and S2). The volume of O_2 consumption, CO_2 production, energy expenditure, and locomotor and ambulatory activity increased in young TG mice compared with control mice (Figures 2C–2H). Calculation of the analysis of covariance (ANCOVA) demonstrated that the energy expenditure for the TG and control mice groups at 10 weeks of age was affected by the amount of lean mass. However, there was no significant group-by-mass interaction. Linear regression analysis, with lean mass as the covariate, showed that energy expenditure was significantly higher in TG mice than in control mice in the dark cycle (Figure 2F) and not in the light cycle (Figure S2O). These data are consistent with the literature that describes FGF21's role in the CNS to stimulate energy expenditure, and the mice lose weight independently of food intake. However, by 1.5 years of HFD, the volume of O_2 consumption and CO_2 production was significantly lower in TG mice (Figures 2I–2L). Aged transgenic mice lacked the increased activity levels seen in young mice (Figures 2M and 2N). ANCOVA and linear regression analysis demonstrated that the energy expenditure between the groups in aged mice was similarly affected by lean mass. Additionally, after adjusting for lean mass, there was no difference between TG and control mice in the dark or light cycles (Figures 2L and S2P). Furthermore, there was no change in systemic fatty acid oxidation after 10 weeks or 1.5 years on HFD, assessed by the respiratory exchange ratio (RER), indicating the TG and control mice used carbohydrates or lipids at comparable proportions for energy production (Figures 2O and 2P). The data above indicate that FGF21 drives significant metabolic benefits early in life via the CNS by increasing activity and energy expenditure. However, energy expenditure by FGF21 is compensated for later in life in aged mice. Thus, in TG mice, the lean body weight, nutrient homeostasis, and antiaging effects are partly due to the peripheral effects of FGF21.

Adipocyte-specific FGF21 overexpression improves glycemic control in aged mice

The development of insulin resistance is considered a hallmark of the aging process. Distinct from its role in energy expenditure, the peripheral insulin-sensitizing effects of FGF21 are primarily mediated by adipose tissue. Aged TG mice did not show increased energy expenditure, so we examined glucose homeostasis in response to elevated circulating FGF21 in young and aged mice fed HFD-dox. TG mice exhibited significantly lower glucose excursion during an oral glucose tolerance test (OGTT) after 16 weeks and 1.5 years of HFD-dox compared with controls (Figures 3A and 3B). Similarly, insulin had a more substantial glucose-lowering effect in an insulin tolerance test (ITT) in TG mice compared with control mice (Figures 3C and 3D).

Along with the improved systemic insulin sensitivity seen in TG mice, basal or glucose-stimulated serum insulin levels were markedly lower than those of control mice (Figures 3E and 3F). Insulin-protein kinase B (PKB; AKT) signaling regulates the metabolism of adipose tissues by promoting glucose utilization, protein synthesis, and lipogenesis. Western blots show that phosphorylated AKT levels were elevated in eWAT and scWAT (Figures 3G and 3H). Histological examination of the adipose tissue revealed smaller adipocytes and fewer crown-like structures that harbor inflammatory macrophages in TG mice compared with control mice (Figure 3I). Peroxisome proliferator-activated receptor gamma ($PPAR\gamma$) is a master regulator of adipogenesis and insulin sensitization in adipocytes. Gene expression for *Pparg* significantly increased in eWAT and scWAT in TG mice compared with control mice (Figure 3J). Adiponectin mRNA levels were significantly increased in eWAT in TG mice fed a HFD for 1.5 years compared with control mice (Figure 3K). Serum adiponectin levels were over 3-fold higher in aged TG mice vs. control mice (Figure 3L). High adiponectin is a signature marker for healthy adipose tissue and insulin sensitivity. These data suggest adipocyte-specific FGF21 overexpression has significant and sustained benefits on eWAT and scWAT function and improvements in whole-body glucose metabolism. Furthermore, these metabolic changes were sustained even after energy expenditure declined, indicating that FGF21 significantly affects peripheral organs in aged mice.

To better understand the cellular mechanisms by which FGF21 influences adipocyte function, we performed quantitative proteomics analysis and qPCR on eWAT and scWAT from mice fed a HFD-dox diet for 1.5 years. The overexpression of FGF21 resulted in a significant remodeling of the proteome, more pronounced in eWAT from aged mice (Figures 3M and S3A–S3F). In both adipose tissue depots, proteins and genes associated with insulin signaling pathways were upregulated, including key metabolic regulators such as *Glut4* (*Slc2a4*), *Pck1*, *Fasn*, and *Acaca* in TG mice compared with controls (Figures 3N–3Q). After 1.5 years of HFD-dox, gene expression for adiponectin (*Adipoq*) and trafficking Regulator of GLUT4 (*Trarg1*) increased 8-fold in eWAT but not in scWAT of TG mice (Figures 3O and 3Q). Genes that regulate glycolysis were upregulated in scWAT, with only 6-phosphofructokinase liver type (*Pfkl*) expression increased in eWAT upon FGF21 overexpression (Figures S3G and S3H). Conversely, the protein levels of rate-limiting glycolytic enzymes, such as PFKL and pyruvate kinase M1/2 (PKM),

(C–H) Indirect calorimetry performed at 22°C in control and TG mice after 10 weeks of HFD-dox ($n = 6$). VO_2 consumption (C), VCO_2 production (D), energy expenditure (E), linear regression for energy expenditure with lean mass as a covariate in the dark phase (F), locomotor activity (G), and ambulatory activity (H). (I–N) Indirect calorimetry performed at 22°C in control and TG mice after 1.5 years HFD-dox ($n = 5–7$). VO_2 consumption (I), VCO_2 production (J), energy expenditure (K), linear regression for energy expenditure with lean mass as a covariate in the dark phase locomotor activity (L), ambulatory activity (M), and locomotor activity (N).

(O–P) Respiratory exchange ratio in control and TG mice fed HFD for 10 weeks (O) ($n = 6$) and 1.5 years (P) ($n = 5–7$).

Error bars represent mean ± SEM. *n* number for (A)–(P) denotes biological replicates. Significance in (A) and (B) between control and TG mice was calculated using a two-tailed Student's t test. Metabolic cage data (C–L) were analyzed by ANCOVA in CalR (https://calrapp.org/) with lean mass as a covariate.[30] See also Tables S1 and S2. Determination of the coefficient of determination (*R*-squared) for (F and L) was determined by linear regression analysis. Differences were considered significant when $p > 0.05$. Not significant (ns), $p > 0.05$, $^{*}p < 0.05$, $^{**}p < 0.01$, $^{***}p < 0.001$, and $^{****}p < 0.0001$.

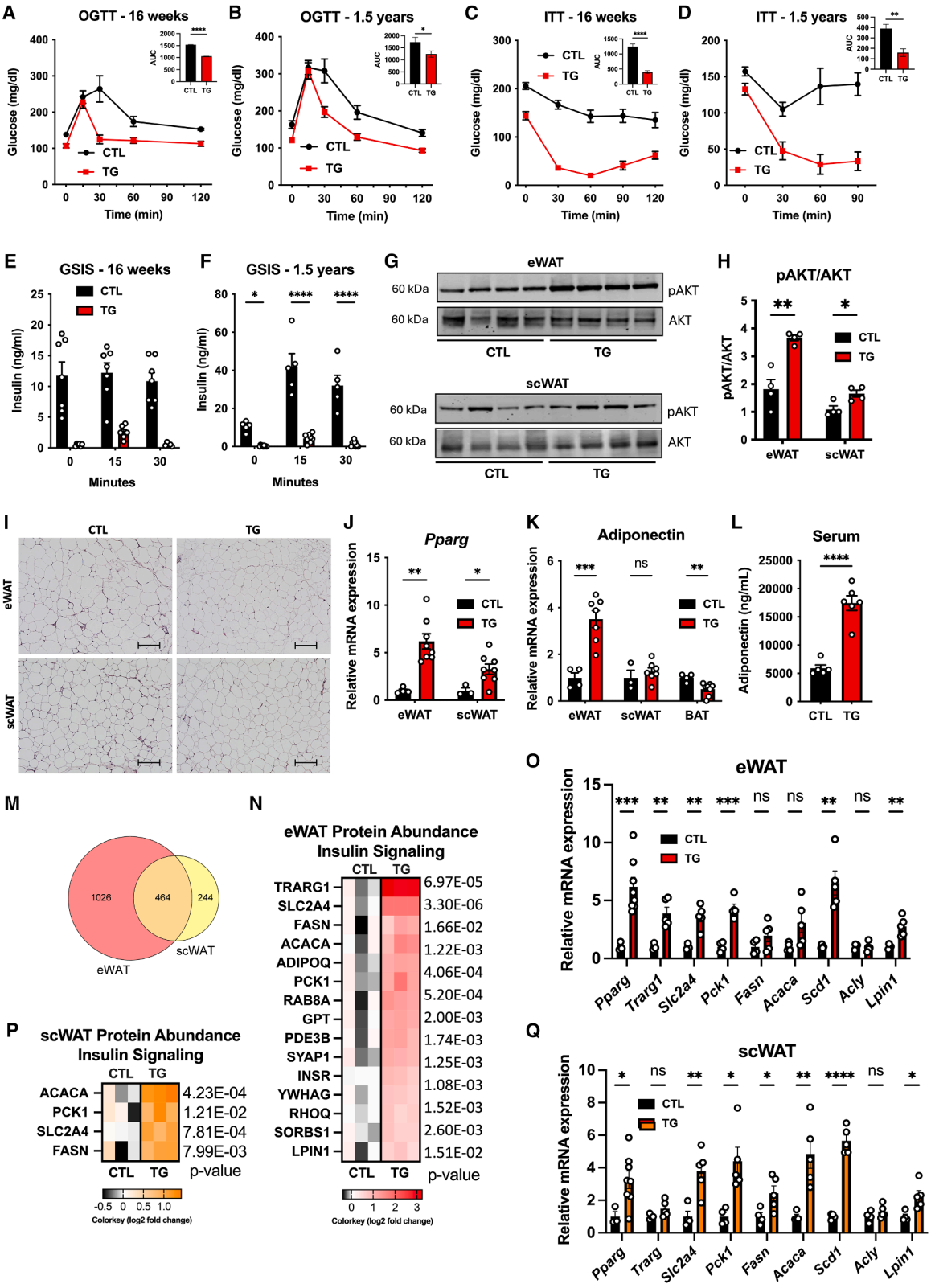

Figure 3. FGF21 overexpression prevents adipose tissue dysfunction and sustains insulin sensitivity in aged mice fed a HFD for 1.5 years

(A and B) OGTT. Inset shows area under the curve (AUC). Male control and TG mice were fed HFD+dox for 16 weeks (A) (n = 6–7) and 1.5 years (B) (n = 11–17). (C and D) ITT. Inset shows area under the curve. Male control and TG mice were fed HFD+dox for 16 weeks (C) (n = 5–7) and 1.5 years (D) (n = 4–6).

(legend continued on next page)

significantly decreased in both eWAT and scWAT (Figures S3I and S3J). Interestingly, the changes in mRNA expression did not correspond with the proteomic data, as illustrated by the divergent results for PFKL and PKM protein and mRNA in eWAT and scWAT (Figures S3I and S3J). These findings underscore the profound and lasting impact of FGF21 overexpression on both eWAT and scWAT insulin sensitivity during aging-induced metabolic stress.

FGF21 overexpression restores lipogenesis in adipocytes during a HFD challenge

In the presence of sufficient glucose, insulin upregulates enzymes that enhance lipogenesis. By contrast, obesity and insulin resistance reduce the lipogenic potential of adipocytes. Since mice with adipose-specific FGF21 overexpression were more insulin-sensitive than control mice, we investigated whether FGF21 overexpression could restore adipocyte lipogenesis and storage of lipids. Figures 4A and 4B and Table S3 illustrate lipid metabolism proteins identified by gene ontology analysis to be altered by FGF21 overexpression in eWAT and scWAT. Proteins that regulate lipogenesis, such as ACACA, FASN, SCD1, and ACLY, were enriched in eWAT and scWAT from TG mice vs. control mice (Figures 4A and 4B). Of these proteins, only gene expression for *Scd1* significantly increased in eWAT, while in scWAT, gene expression for *Scd1*, *Fasn*, and *Acaca* increased (Figures 3O and 3Q). Increased lipogenesis is observed in the mice with FGF21 overexpression. When fat mass is expressed as % of body weight, the TG mice have larger eWAT mass and equal scWAT mass to controls (Figures 1N and 1O). Interestingly, even without correcting for body weight, the eWAT fat pad mass is the same for control and TG mice.

Enhanced rates of triglyceride breakdown (lipolysis) are associated with elevated free fatty acids taken up by other tissues. To functionally determine if FGF21 affects the activation of lipolysis adipose tissue, we administered a β3-adrenergic receptor agonist, which stimulates lipolysis specifically in adipocytes. In response to the agonist, the levels of the end products of lipolysis, serum non-esterified fatty acids (NEFAs), and glycerol were reduced in TG mice compared with control mice (Figures 4C and 4D). Basal serum NEFA levels were lower in aged TG mice vs. controls (Figure 4E).

Many short-term studies demonstrate that FGF21 promotes insulin sensitivity in adipose tissue. By investigating aged mice fed a HFD for 1.5 years, we determined that continuous overexpression of FGF21 can increase lipogenesis and lower lipolysis in adipose tissue, potentially improving systemic lipid metabolism.

FGF21 protects against HFD-induced hepatic steatosis in aged mice

Many current models suggest that adipose tissue dysfunction leads to ectopic fat deposition in the liver, hepatic lipotoxicity, and metabolic dysfunction-associated fatty liver disease (MAFLD) with aging. Pharmacological FGF21 profoundly alleviates steatosis, liver inflammation, and fibrosis, prompting us to examine adipocyte-derived FGF21's role in liver function.[8,31] Serum cholesterol and triglycerides were lower in aged TG mice compared with controls (Figures 4F and 4G). Microscopically, the aged livers from control mice showed significant microvesicular steatosis by H&E staining, which remained resolved in TG mice even after 1.5 years of HFD-dox (Figure 4H). Serum markers of liver dysfunction, aspartate aminotransferase (AST) and alanine transaminase (ALT), were unchanged upon adipocyte-specific FGF21 overexpression after 16 weeks of HFD but were significantly reduced in response to FGF21 overexpression by 6 months and 1.5 years of age (Figures 4I, S4A, and S4B). Additionally, the expression of genes associated with fibrosis was reduced in the liver when FGF21 was overexpressed in adipose tissue (Figure 4J). These results indicate a role of FGF21 in liver steatosis independent of fat mass, which plateaued in TG mice by 16 weeks, but the effects on AST and ALT did not occur until later in the mouse's life.

We then examined whether the liver was affected by increased circulating FGF21 from adipose tissue. Previous studies show that pharmacological or liver-specific FGF21 overexpression promoted gluconeogenesis, oxidation of free fatty acids, and ketogenesis in the liver.[4] In our transgenic mouse model fed a HFD, canonical genes that regulate *de novo* lipogenesis in the liver did not change compared with control mice (except for *Scd1*) (Figure 4K). Expression of fatty acid transport genes *Cd36* decreased, and *Fatp1* increased in TG mice compared with control mice. FGF21 regulates *Abca1*, which was increased in TG mice. Other essential receptors expressed in the liver, *Ldlr*

(E and F) Serum insulin levels after 2 g/kg glucose administration. Control and TG mice were fed HFD-dox for 16 weeks (E) (n = 5–7) and 1.5 years (F) (n = 5–9).
(G) Western blots for phosphorylated AKT protein expression relative to total AKT in mice fed HFD-dox for 1.5 years (n = 4).
(H) Quantification of (G) (n = 4).
(I) H&E staining of eWAT and scWAT depots of control and TG mice fed on HFD-dox for 1.5 years. Scale bar 200 μM.
(J) *Pparg* mRNA expression in eWAT (n = 4–8) and scWAT (n = 3–8).
(K) Adiponectin mRNA levels relative to control in eWAT, scWAT, and BAT (n = 4–13).
(L) Serum adiponectin levels in control and TG mice fed on HFD-dox 1.5 years (n = 5–6).
(M) Venn diagram for the number of significantly different proteins altered by FGF21 overexpression compared with control mice in eWAT and scWAT (n = 3).
(N) Heatmap displaying Z score normalized protein expression as $\log_2$FC for insulin signaling proteins increased in eWAT from control and TG mice identified as significant by GO enrichment analysis for biological processes (n = 3).
(O) mRNA expression for insulin signaling responsive genes in eWAT (n = 4–5).
(P) Heatmap displaying Z score normalized protein expression as $\log_2$FC for insulin signaling proteins increased in scWAT from control and TG mice identified as significant by GO enrichment analysis for biological processes (n = 3).
(Q) mRNA expression for insulin signaling responsive genes in scWAT (n = 4–5).
Error bars represent mean ± SEM. n, number for (A–Q), denotes biological replicates. Significance for AUC (A–D) compared between groups using independent samples t test. Significance in (E), (F), (H), (J)–(L), (O), and (Q) between control and TG mice was calculated using a two-tailed Student's t test. Error bars represent mean ± SEM not significant (ns), $p > 0.05$, $^{*}p < 0.05$, $^{**}p < 0.01$, $^{***}p < 0.001$, and $^{****}p < 0.0001$. Statistical significance for the relative abundance of quantified proteins (N and P) was determined by a two-tailed Student's t test in between control and TG mice. The significant cutoff criterion for GO enrichment analysis (N and P) was false discovery rate (FDR) < 0.05 (adjusted p value for multiple comparisons by the Benjamini-Hochberg procedure).

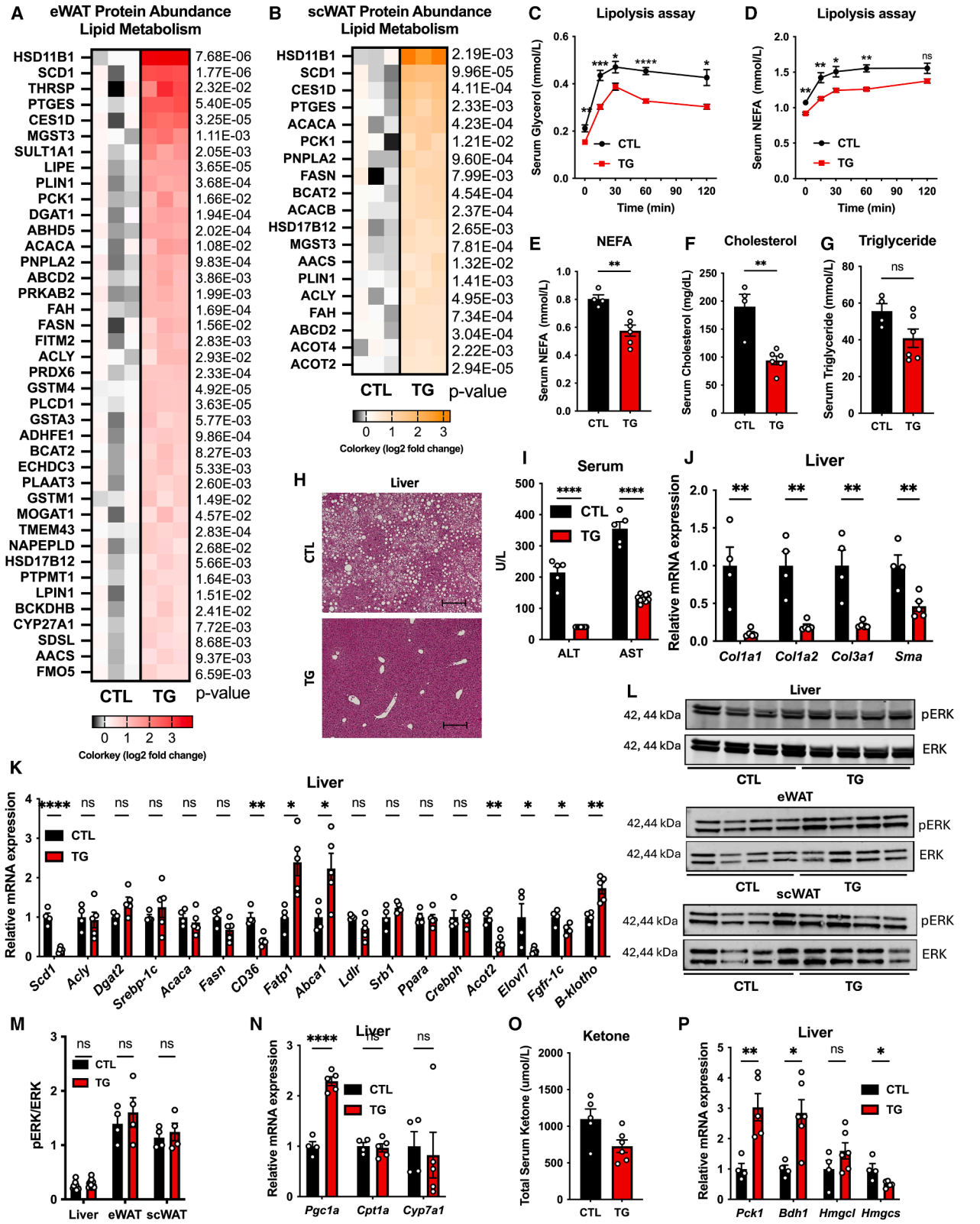

(legend on next page)

and *Sr-b1*, were unchanged between the groups. *Fgf21* mRNA levels are significantly lower in the liver upon FGF21 overexpression in the adipose tissue. Other mediators that stimulate Fgf21 expression in the liver are *Ppara* (fasting) and *Crebph* (carbohydrate intake), but neither mRNA was changed in the liver in TG mice compared with control mice. Interestingly, other PPARa targets, *Acot2* and *Elovl7*, were significantly reduced in the livers of TG mice (Figure 4K). The receptors that mediate FGF21 signaling were significantly affected by adipocyte-specific overexpression of FGF21. *Fgfr1c* decreased, and β-*klotho* increased in the transgenic mice vs. control mice (Figure 4K). FGF21 signaling via FGFR1c/β-klotho activates mitogen-activated protein kinase (MAPK) and the extracellular signal-regulated kinase (ERK) pathway, which regulates glucose uptake and energy metabolism. Basal ERK signaling was not significantly altered in the liver, eWAT, or scWAT (Figures 4L and 4M). These data contrast with how FGF21 overexpression stimulated basal pAKT/AKT in eWAT and scWAT (Figures 3G and 3H). Chronic obesity has been shown to elevate ERK phosphorylation in adipose tissue, which may impair FGF21 signaling in aged mice fed a HFD. FGF21 has previously been shown to regulate hepatic expression of FA oxidation genes (*Cpt1a*, *Ppara*, and *Pgc1a*) and bile acid synthesis genes (*Cyp7a1*).[31,32] However, only *Pgc1a* gene expression increased in mice with adipocyte-specific overexpression of FGF21 (Figures 4K and 4N). Therefore, reducing liver steatosis in mice by overexpressing FGF21 may lower lipid mediators.

Prior studies suggest that FGF21 overexpression causes growth retardation and induces ketogenesis.[19,23] Adipocyte-specific, inducible FGF21 overexpression did not increase ketogenesis in the liver, as judged by the lower circulating total ketones in TG mice (Figure 4O). This is consistent with the elevated phosphoenolpyruvate carboxykinase (PEPCK; *Pck1*) gene expression in the liver from transgenic mice vs. control mice (Figure 4P). As the rate-limiting enzyme in gluconeogenesis, high PEPCK activity decreases fatty acid oxidation and, consequently, lowers ketone body production. In addition, the expression for the ketogenesis gene 3-hydroxy-3-methylglutaryl-CoA synthase 1 (*Hmgcs*) decreased in liver tissue from TG mice, while 3-hydroxybutyrate dehydrogenase 1 (*Bdh1*) increased, and no change was seen for 3-hydroxy-3-methylglutaryl-CoA lyase (*Hmgcl*) (Figure 4P). Collectively, our data indicate that FGF21 affects hepatic metabolism differently if expressed in another tissue in the context of aged mice. Overall, the collected results show that the elevation of adipocyte FGF21 in the context of HFD improved liver function in aged mice, primarily by lowering hepatic lipid content.

Cold-stress-induced thermogenesis is not altered by adipocyte FGF21 overexpression in obese mice

Previous reports show that FGF21 activates thermogenic adipocytes in BAT and scWAT, which improves cardiometabolic health.[26,33] In our mouse model of adipocyte-specific overexpression of FGF21, the mRNA and protein expression of FGF21 increased in BAT and scWAT compared with controls (Figures 1E and S1C). Therefore, we assessed whether thermogenic gene expression in BAT or scWAT was induced by FGF21. Compared with control mice, overexpression of FGF21 in scWAT did not change *Ucp1* gene expression but stimulated the expression of canonical mediators of thermogenesis, *Ppary* and *Ppargc1a* (Figure S4C). In the BAT of TG mice, there was an increase in thermogenic gene expression (*Ucp1*, *Cidea*, and *Dio2*) (Figure S4F). Cold stimulation increases the expression of *de novo* lipogenesis genes in BAT, which increased in response to FGF21 overexpression in BAT (*Fasn*, *Agpat2*, and *Dgat2*) (Figure S4F). Surprisingly, adiponectin mRNA decreased in the BAT of TG mice compared with control mice (Figure 3K). Histological analyses highlight that BAT was significantly delipidated, and the tissue weight was decreased in aged TG mice vs. controls (Figures S4D and S4E). Additionally, scWAT adipocytes were smaller in TG mice vs. control mice, displaying no signs of beiging (Figure 3I).

Brown or beige adipocyte thermogenesis is acutely influenced by ambient temperature. To assess whether adipocyte-derived FGF21 promoted cold tolerance during obesity, we performed indirect calorimetry in mice exposed to 6°C over the course of 24 h. The HFD-dox feeding was limited to 10 weeks to ensure brown adipose tissue was functional. At 6°C and adjusting for lean mass, the TG mice displayed increased O_2 consumption, CO_2 production, and energy expenditure compared with control mice (Figures S4G–S4I; Table S1). Linear regression analysis determined that lean mass affected energy expenditure similarly in the two groups (Figures S4H and S4I). RER did not differ at 22°C between control and TG mice (Figure 2O). However, at 6°C, RER was higher in TG mice than in the controls during the

Figure 4. Adipocyte-specific FGF21 overexpression preserves white adipose tissue lipid metabolism and prevents liver steatosis in mice fed a HFD for 1.5 years

(A and B) Heatmaps displaying *Z* score normalized protein expression as $\log_2$FC for increased lipid metabolism proteins from control and TG mice were identified as significant by GO enrichment analysis for biological processes in eWAT (A) ($n = 3$) and scWAT (B) ($n = 3$).

(C and D) Control and TG mice were fed HFD-dox for 8 weeks. Beta-3 adrenergic receptor agonist (CL 316 and 243) and blood were collected at 0, 15, 30, 60, and 120 min. Serum glycerol (C) ($n = 6$–8) and NEFA (D) ($n = 6$–8).

(E–L) Control and TG mice were fed HFD+dox for 1.5 years. Serum NEFA (E) ($n = 4$–6), cholesterol (F) ($n = 4$–6), and triglyceride (G) ($n = 4$–6). (H) H&E staining of liver tissue. Scale bar, 100 μM. (I) Serum ALT and AST ($n = 5$–9). (J) mRNA expression for fibrosis genes in liver ($n = 4$–5). (K) mRNA expression for lipid metabolism genes and FGF21 receptors (*Fgfr1c* and *β-klotho*) in liver ($n = 4$–5). (L) Western blots for phosphorylated ERK protein expression relative to total ERK in mice fed HFD-dox 1.5 years ($n = 4$).

(M) Quantification of (L) ($n = 4$).

(N) mRNA expression for FA oxidation genes (*Cpt1a*, *Ppara*, and *Pgc1a*), and bile acid synthesis genes (*Cyp7a1*) in the liver ($n = 4$–5).

(O) Serum total ketone levels ($n = 5$–6).

(P) mRNA expression for ketogenesis-associated genes in liver ($n = 4$–5).

n number for (A)–(P) denotes biological replicates. Significance in (A), (B), (E)–(G), (I)–(K), and (M)–(P) between control and TG mice was calculated using a two-tailed Student's t test. The significance between control and TG mice for (C) and (D) was calculated by two-way ANOVA. Error bars represent mean ± SEM not significant (ns), $p > 0.05$, $^{*}p < 0.05$, $^{**}p < 0.01$, $^{***}p < 0.001$, and $^{****}p < 0.0001$).

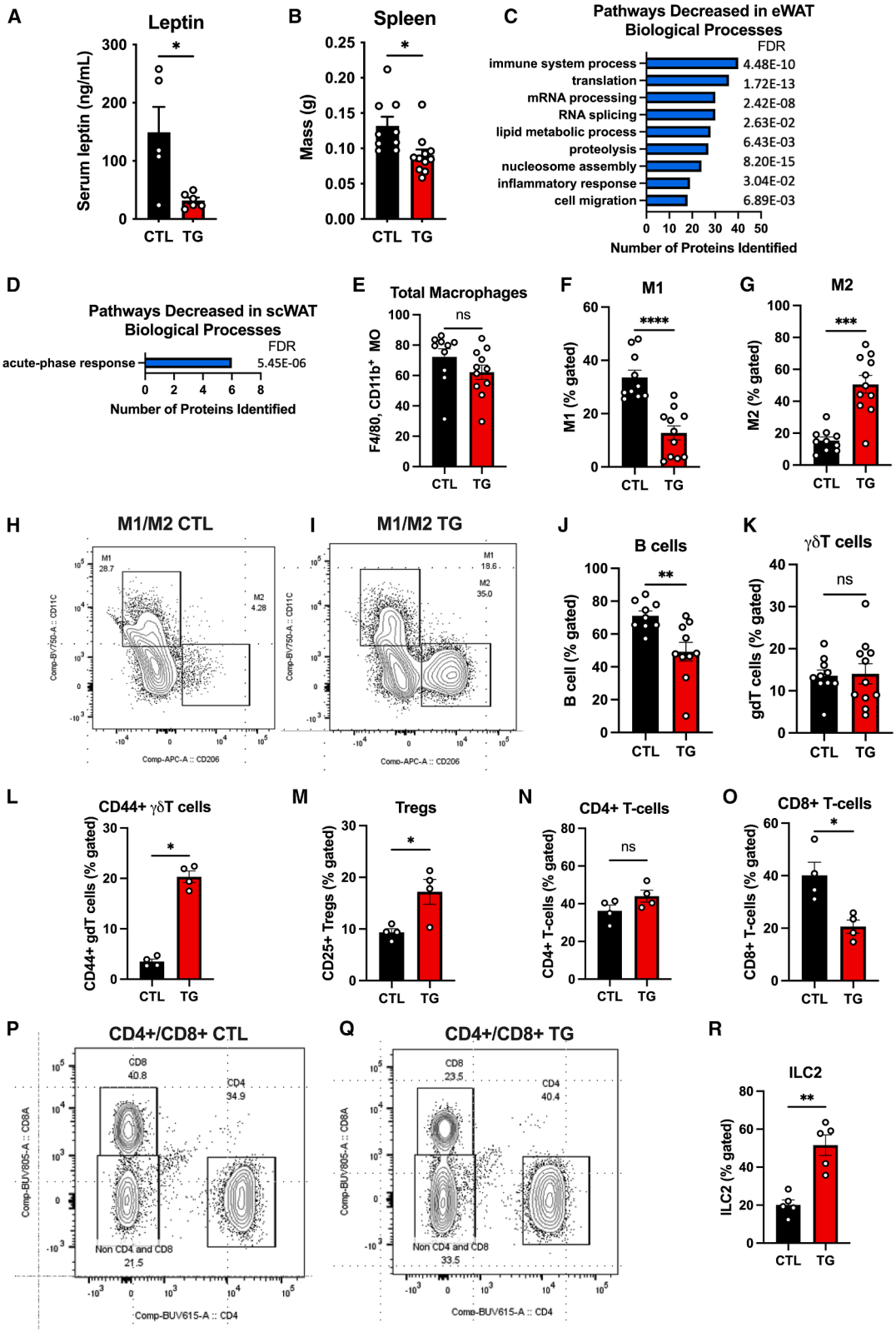

Figure 5. FGF21 overexpression promotes improved immunometabolism in visceral adipose tissue in aged mice fed a HFD

(A–D) Control and TG mice were fed HFD+dox for 1.5 years beginning at 10–12 weeks of age. Serum leptin (A) (n = 5–6). Spleen weight (B) (n = 9–11). GO enrichment analysis for decreased proteins (biological processes) in eWAT (C) and scWAT (D) (n = 3).

(legend continued on next page)

light phase, indicating FGF21 overexpression promoted the use of carbohydrates as fuel in response to cold (Figure S4J; Table S1). We also tested whether FGF21 promoted energy expenditure at thermoneutrality (30°C), which is a condition that minimizes BAT activity. O_2 consumption, CO_2 production, and energy expenditure in the light phase were significantly *increased* in TG mice compared with control mice, with no differences in RER (Figures S4K–S4N; Table S1). Locomotor activity between control and transgenic mice did not differ if exposed to either 30°C or 6°C (Figures S4O and S4P; Table S1). We conclude that although FGF21 stimulates thermogenic gene expression in scWAT and BAT, TG mice do not increase functional cold-stress-induced thermogenesis compared with control mice in the context of obesity. Since the induction of adipocyte-specific overexpression promoted energy expenditure at thermoneutrality, FGF21's action in the context of its adipocyte-specific overexpression is, in part, independent of BAT function, a somewhat surprising result considering the high level of FGF21 overexpression in BAT.

FGF21 expression prevents adipose tissue inflammation

Adipose tissue is an organ with major immunological activity during aging-obesity and exhibits characteristics of both innate and adaptive immune responses.[34–37] Cytokines released by adipocytes or infiltrating macrophages drive low-grade chronic inflammation, leading to insulin resistance and associated diseases of obesity and aging.[34–37] Leptin is a pro-inflammatory adipokine that is typically elevated in obesity and contributes to chronic low-grade inflammation. In TG mice, serum leptin levels were reduced to one-third of those observed in control mice (Figure 5A). Further evidence of reduced systemic inflammation in TG mice includes a significant reduction in spleen weight at 1.5 years of age, consistent with decreased systemic immune activation (Figure 5B).

Proteomic Gene Ontology (GO) analysis in aged TG mice revealed a marked reduction in proteins associated with immune response pathways, particularly in the eWAT of the transgenic mice (Figures 5C and S5A; Table S3). These changes in the proteome were primarily observed in eWAT, with scWAT showing only one change in the biological processes category and no changes in the molecular function category in the transgenics, suggesting a depot-specific effect of FGF21 on immune function in adipose tissue (Figure 5D; Table S3). Macrophages are the most abundant immune cell type in adipose tissue during obesity and are fundamental to initiating and sustaining inflammatory responses.[35] After 1.5 years of HFD-dox feeding, total macrophage numbers in eWAT did not differ between TG and control mice (Figure 5E). However, there was a significant shift in macrophage subtypes indicative of an inflammatory response. Specifically, FGF21 overexpression led to a decrease in M1-like pro-inflammatory macrophages and an increase in M2-like anti-inflammatory macrophages (Figures 5F–5I).

Aging is associated with aberrant expansion of effector memory cells, the loss of naive T lymphocytes,[2,9] and an expansion of adipose B cells.[38] FGF21 protects against thymic involution by improving thymic epithelial cell function, which is crucial for maintaining T lymphocyte development.[9,39] In this study, overexpression of FGF21 in eWAT decreased B cell frequency (Figure 5J) with a reduction in CD8 cells without affecting the CD4 frequencies (Figures 5N–5Q). These data are consistent with the studies demonstrating that the depletion of adipose tissue B cells restores insulin sensitivity in aged mice.[38] FGF21 overexpression in TG mice did not affect the natural killer cells between the groups (Figure S5B). Interestingly, despite the association of diet-induced obesity with an increase in gamma delta T cells (γδT cells), no changes in total γδT cell numbers were observed between TG and control mice (Figure 5K).[40] However, a specific increase in pro-inflammatory $CD44^+$ γδT cells was noted in eWAT from the TG mice compared with controls (Figure 5L). This suggests a nuanced role of FGF21 in modulating γδT cell activity, potentially balancing immune responses during aging.

It was previously reported that Tregs are depleted during obesity,[41] while elevated Tregs in adipose tissue in aging mice contribute to metabolic stress and insulin resistance.[42,43] Interestingly, aged TG mice fed chronic HFD displayed higher Tregs in visceral adipose tissue (Figure 5M) compared with control mice, which is associated with decreased inflammation and metabolic dysregulation.[44,45] In addition, FGF21 overexpression led to an increase in group 2 innate lymphoid cells (ILC2s) in adipose tissue of aged TG mice fed a HFD (Figure 5R). Given that ILC2 numbers typically decrease in adipose tissue during obesity, this increase further emphasizes FGF21's role in promoting an anti-inflammatory immune environment.[46] The immunomodulatory aspects of FGF21 have not been previously observed in the adipose tissue of aged mice. These data show that FGF21 maintains tissue-resident immune cell homeostasis within adipose tissue, even in old mice, reducing "inflammaging."

FGF21 reduces ceramide levels in visceral adipose tissue

Next, we investigated the potential mechanisms by which FGF21 promotes anti-inflammatory effects in visceral adipose tissue. The co-receptor for FGF21, βKlotho, is not expressed in macrophages or T cells, indicating that FGF21's impact on immunometabolism likely occurs indirectly through its action on cells within the adipose tissue niche.[9] FGF21 reduces the levels of ceramides, bioactive lipid metabolites that increase in metabolic tissues during obesity and induce cellular dysfunction by inhibiting insulin signaling and other mechanisms (Figure 6A).[47,48] Evidence shows that specific circulating ceramide species are biological predictors and markers of cardiovascular disease, atherosclerosis, and type

(E–R) Flow cytometry for the proportion of immune cells in eWAT from control and TG mice fed HFD-dox for 1.5 years. Total macrophages (E) (n = 10–11), M1 macrophages (F) (n = 10–11), and M2 macrophages. (G) (n = 10–11). Representative gating strategy to identify M1 and M2 macrophages (H and I). B cells (n = 9–10) (J). γδT cells (n = 10–11) (K). CD44+ γδT cells (L) (n = 4). CD25+ Tregs (M) (n = 4). CD4+ T cells (N) (n = 4). CD8+ T cells (n = 4) (O). Representative gating strategy to identify CD4+ and CD8+ T cell populations (P and Q). ILC2 cells (n = 5) (R).

n number for (A)–(R) denotes biological replicates. Significance in (A), (B), and (E)–(R) between control and TG mice was calculated using a two-tailed Student's t test. Error bars represent mean ± SEM not significant (ns), $p > 0.05$, *$p < 0.05$, **$p < 0.01$, ***$p < 0.001$, and ****$p < 0.0001$. The significant cutoff criterion for GO enrichment analysis (C and D) was FDR < 0.05 (adjusted p value for multiple comparisons by the Benjamini-Hochberg procedure).

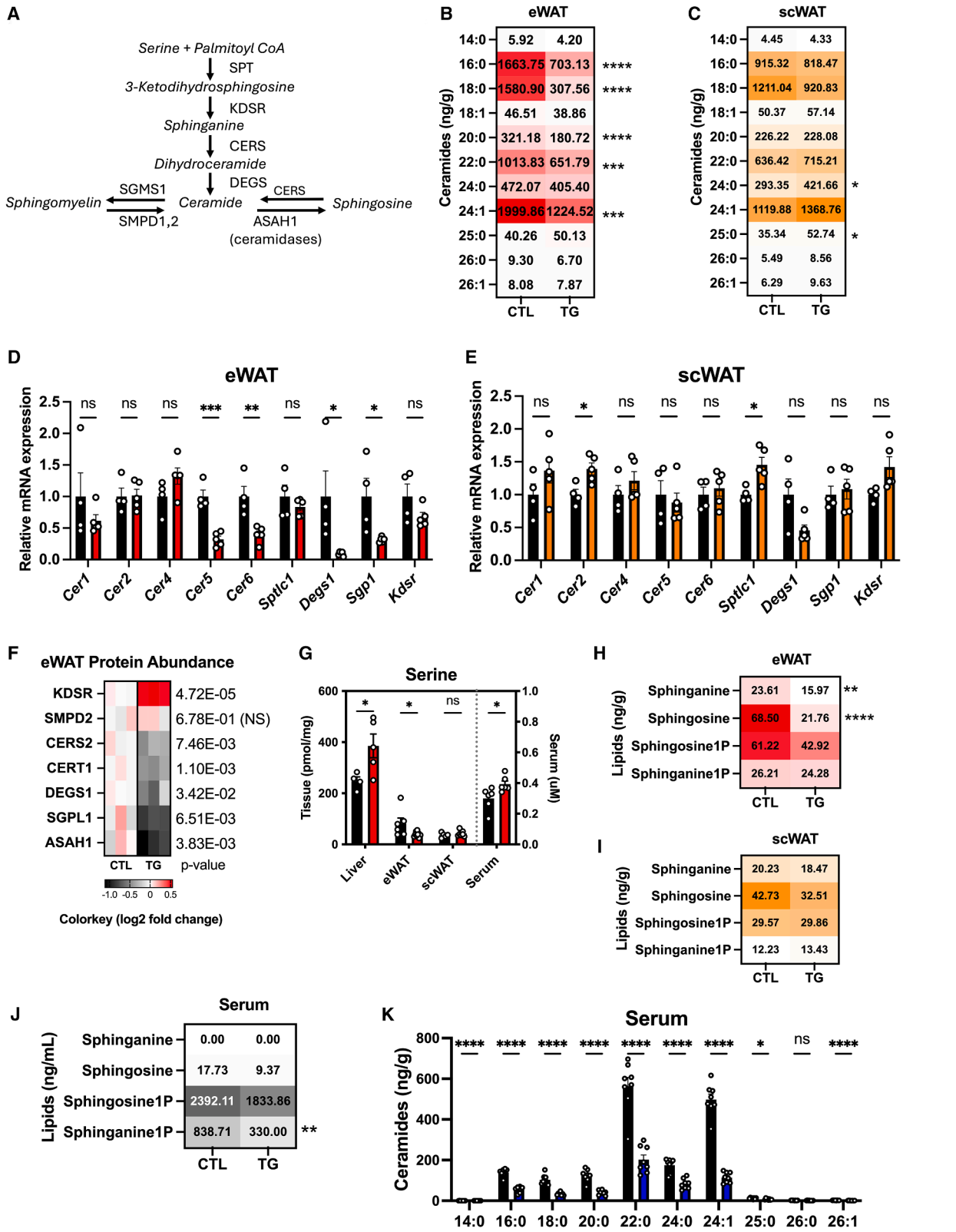

(legend on next page)

2 diabetes.[49] However, how FGF21 alters specific species of ceramides and sphingolipids has not been investigated to date. To determine whether adipocyte-specific FGF21 overexpression alters ceramide profiles in adipose tissue from aged mice fed a HFD, we conducted liquid chromatography-tandem mass spectrometry (LC-MS/MS) analysis.[50] We observed a significant reduction in several ceramide species (C16, C18, C20, C22, and C24:1) in eWAT from FGF21-overexpressing mice (Figure 6B). Conversely, in scWAT from TG mice, ceramides C24 and C25 were elevated compared with control mice (Figure 6C). Gene expression analysis revealed a decrease in ceramide synthase genes, *Cer5*, *Cer6*, and *Degs* decreased in eWAT from TG mice, while expression of *Cer2* and *Sptlc1* was upregulated in scWAT (Figures 6D and 6E). Additionally, eWAT from TG mice showed significant changes in proteins that regulate ceramide metabolism, including an increase in 3-keto-dihydrosphignosine reductase (KDSR) and a decrease in ceramide synthase 2 (CERS2), ceramide transporter 1 (CERT1), delta 4-desaturase (DEGS), sphingosine 1 phosphate lyase (SGPL1), and N-acylsphingosine amidohydrolase 1 (ASAH1) (Figure 6F). There were no changes in the expression levels of proteins involved in ceramide metabolism in scWAT.

The first step in ceramide biosynthesis is the condensation of palmitoyl-coenzyme A (CoA) and serine by serine palmitoyltransferase, producing sphinganine (dihydrosphingosine) (Figure 6A). Serine and sphinganine decreased in eWAT of aged TG mice compared with controls, but this did not occur in scWAT (Figures 6G–6I). In addition, there were no significant differences in the abundance of dihydroceramide intermediates between control and TG mice in either eWAT or scWAT (Figures S6A and S6B).

Alternatively, ceramides can be synthesized or catabolized via sphingosine or sphingomyelin pathways. In TG mice, FGF21 overexpression decreased sphingosine levels in eWAT, with no corresponding change observed in scWAT (Figures 6H and 6I). Moreover, FGF21 overexpression significantly remodeled the sphingomyelin profile across various tissues, including serum, eWAT, scWAT, and liver (Table S4). In eWAT from TG mice, multiple sphingomyelin species, particularly polyunsaturated ones (C16, C16:1, C18, C18:1, C18:2, C18:3, C20:1, C20:2, 22:1, and C24:1), were markedly decreased (Table S4). Conversely, in scWAT, sphingomyelin species C14 and C24 increased, while C16:1, C18, and C18:1 decreased (Table S4). These findings suggest that ceramides are attenuated in eWAT but remain relatively unaltered in scWAT of TG mice. This suggests that FGF21 signaling, specifically in visceral fat, regulates ceramide levels, and this reduction of ceramides persists during aging while exposed to a HFD.

FGF21 reduces sphingolipids in adipose tissue

Ceramides serve as precursors for synthesizing complex glycosphingolipids, such as hexosyl- and lactosyl-ceramides. These bioactive sphingolipids accumulate in various organs during aging and are associated with numerous pathologies.[51,52] In response to FGF21 overexpression, hexosyl- and lactosyl-ceramides (C14, C16, C18, C20, C24, and C24:1) were significantly reduced in eWAT (Figures S6C and S6E). In scWAT, hexosyl-ceramide C16 and lactosyl-ceramides C16, C20, and C22 were also reduced in TG mice compared with controls (Figures S6D and S6F). Furthermore, adipocyte-specific FGF21 overexpression decreased levels of several serum hexosyl- and lactosyl-ceramide species (Figures S6G and S6H). This reduction in ceramides may underlie the anti-inflammatory effects of FGF21, as these sphingolipids are linked to oxidative stress and inflammation. Interestingly, the reduction in hexosyl- and lactosyl-ceramides was most pronounced in eWAT, the adipose depot that also showed the largest decrease in ceramides. The precise mechanisms by which FGF21 regulates these lipid levels warrant further investigation.

Adipose tissue-derived FGF21 decreases circulating ceramide levels in gerobese mice

Elevated concentrations of circulating ceramides are also linked to aging and a higher incidence of cardiovascular disease, stroke, and type 2 diabetes.[49] We investigated whether ceramides that correlate with cardiovascular disease and insulin resistance (C16, C18, C18:1, C24, and C24:1) were altered in serum due to elevated FGF21 levels.[53] In mice fed a HFD for 1.5 years, FGF21 overexpression in adipose tissue decreased the serum levels of ceramide species (C14, C16, C18, C20, C22, C24, C24:1, C25, and C26:1) and sphinganine 1 phosphate compared with control mice (Figures 6J and 6K).

The liver contains high concentrations of ceramides, which can reflect or contribute to systemic ceramide metabolism or distribution.[54] The liver did not display differences in sphingosine or sphinganine in TG mice, and no changes in hexosyl- and lactosyl-ceramides were observed (Figures S6I–S6K). By contrast, ceramides (C20 and C22) and dihydroceramides C22 decreased in the livers of transgenic mice, reflecting decreases observed in the serum (Figures S6L and S6M). Ceramides (C24, C25, and C26) increased in the livers of transgenic mice (Figure S6M). The expression of ceramide metabolism genes showed that only Cers5 decreased in response to FGF21 overexpression (Figure S6N). Generally, *de novo* ceramide synthesis in the liver can strongly affect the serum sphingolipid profile. However, in this genetic model, the data suggest that lower ceramide levels in adipose tissue contribute to lower circulating ceramides.

Figure 6. Adipocyte-specific FGF21 overexpression reduces sphingolipid and ceramide levels in visceral adipose tissue and in circulation in aged mice fed a HFD

(A) Ceramide *de novo* synthesis pathway diagram. SPT, serine palmitoyltransferase; KDSR, 3-keto-dihydrosphignosine reductase; CERS, ceramide synthase; DEGS, delta 4-desaturase; SGMS1, sphingomyelin synthase 1; SMPD1 and 2, sphingomyelin phosphodiesterase 1 and 2; ASAH1, N-acylsphingosine amidohydrolase 1.

(B–K) Male control and TG mice were fed HFD+dox for 1.5 years. (B) Heatmap of ceramide levels in eWAT (n = 6–9). (C) Heatmap of ceramide levels in scWAT (n = 5–9). (D) mRNA expression for ceramide metabolism genes in eWAT (n = 4–5). (E) mRNA expression for ceramide metabolism genes in eWAT. (n = 4–5). (F) Heatmap displaying Z score normalized protein expression as $\log_2$FC for ceramide metabolism in eWAT (n = 3). (G) Tissue and serum levels of serine (n = 4–9). (H–J) Heatmap for sphingolipid levels in eWAT (H) (n = 6–9), scWAT (I) (n = 5–9), and serum (J) (n = 6–9). (K) Ceramide levels in serum (n = 8).

n number for (B)–(K) denotes biological replicates. Significance in (B)–(E) and (F)–(K) between control and TG mice was calculated using a two-tailed Student's t test. Error bars represent mean ± SEM not significant (ns), $p > 0.05$, $^{*}p < 0.05$, $^{**}p < 0.01$, $^{***}p < 0.001$, and $^{****}p < 0.0001$.

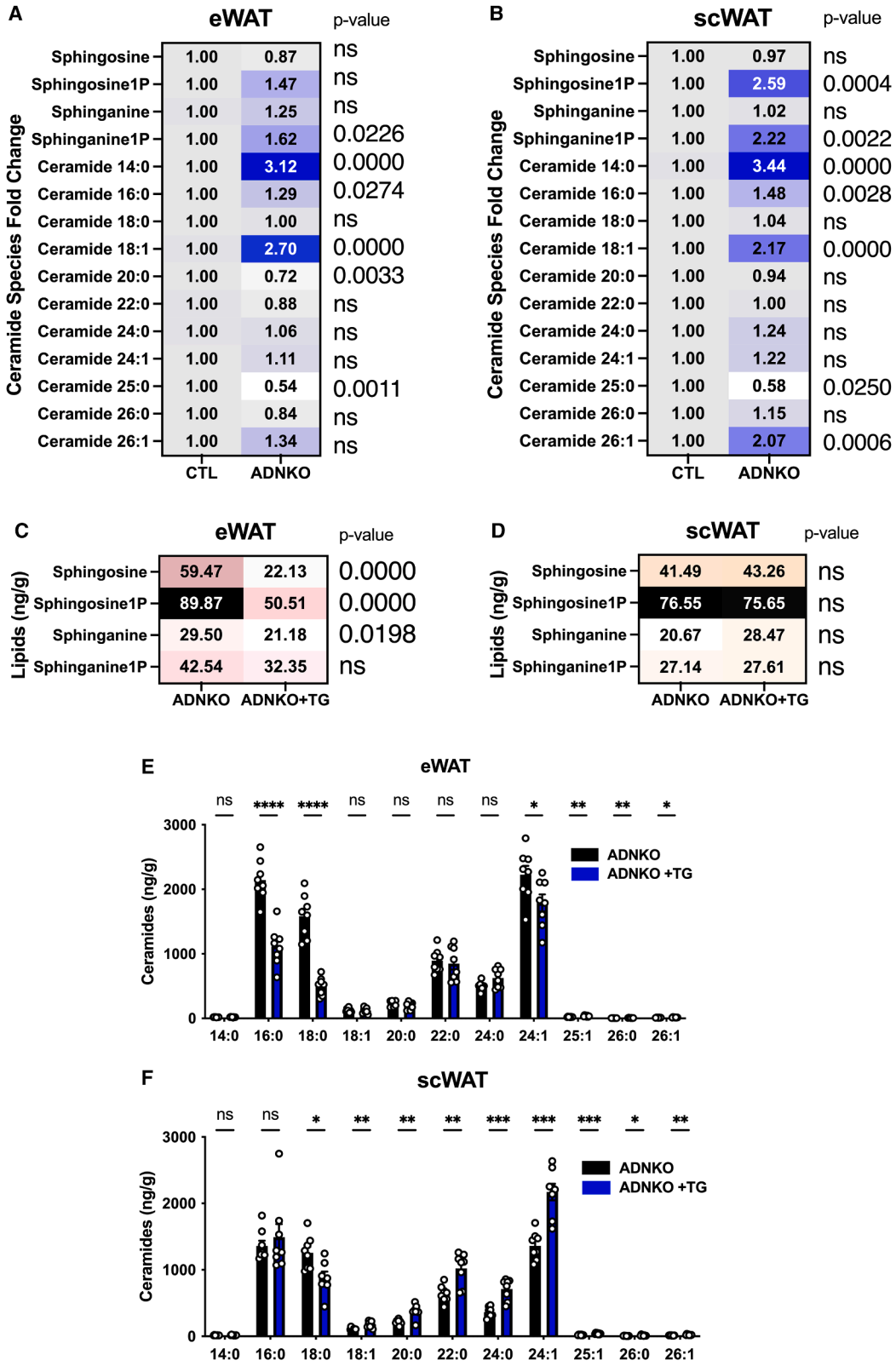

Figure 7. Increases in visceral adipose tissue ceramides in ADNKO mice can be rescued by FGF21 overexpression

(A and B) Ceramide species in control and adiponectin knockout mice (ADNKO) male mice fed HFD+dox for 1.5 years expressed as fold change in eWAT (A) (n = 5–8) and in scWAT (B) (n = 5–8).

(legend continued on next page)

FGF21 reduces ceramides in visceral fat independently of adiponectin

Overexpression of FGF21 in adipocytes robustly increased serum adiponectin levels, a potent anti-inflammatory mediator (Figure 3L). Notably, adiponectin receptors possess intrinsic ceramidase activity, which facilitates the breakdown of ceramides—lipotoxic damage-associated molecular pattern (DAMP) implicated in age- and obesity-related inflammasome activation,[55,56] insulin resistance, diabetes, and cardiovascular disease in both humans and non-human primates.[49] The lipid excess associated with obesity drives *de novo* ceramide synthesis, further exacerbating metabolic dysfunction.[57] Our data suggest that FGF21 may reduce ceramide levels through several mechanisms, including decreasing the availability of serum free fatty acids, establishing an anti-inflammatory environment within adipose tissue, and modulating signaling pathways that regulate the expression of genes and proteins involved in ceramide synthesis or degradation. Given that FGF21's effects on adipose tissue have been shown to be mediated by adiponectin,[47] we hypothesized that adiponectin plays a crucial role in FGF21's ability to reduce tissue ceramide levels in this setting.

To investigate this, we bred adiponectin knockout (ADNKO) mice previously generated in our lab with transgenic mice that were heterozygous for adiponectin promoter-driven rtTA and TRE-FGF21, resulting in ADNKO mice with or without adipocyte-specific FGF21 overexpression.[58] All mice were fed HFD-dox for 1.5 years. Compared with the control mice, ADNKO mice exhibited increased levels of sphingolipids in eWAT and scWAT (Figures 7A, 7B, S7A, and S7B). When FGF21 was inducibly overexpressed in mice on the ADNKO background, sphingolipids were significantly reduced, primarily in eWAT (Figures 7C and 7D). Moreover, levels of several ceramide species significantly decreased in the eWAT of ADNKO mice with FGF21 overexpression (Figures 7E and 7F). By contrast, ceramide levels increased in scWAT in ADNKO mice with FGF21 overexpression vs. ADNKO control mice.

Ceramide levels in eWAT and scWAT increased when adiponectin was absent, which is consistent with our previous observations that adiponectin has potent anti-lipotoxic effects in adipose tissue. Notably, eWAT was particularly sensitive to FGF21 signaling and displayed lower ceramide levels than scWAT. In eWAT, this occurs even in the absence of adiponectin. By contrast, scWAT remains sensitive to the lack of adiponectin, leading to increased ceramide levels in the presence of FGF21. This suggests that FGF21 signaling and the crosstalk with adiponectin in eWAT and scWAT differ. How FGF21 signals in eWAT is an important aspect of how adipose tissue contributes to obesity and aging and reinforces its potential that adipose tissue has as a therapeutic target for metabolic disorders. FGF21-stimulated increases in energy expenditure were lost in aged mice, indicating that the ceramide-lowering ability of FGF21 plays a role in lifespan extension. Collectively, our data underscore the complexity and significant metabolic effects of the FGF21-adiponectin-ceramide axis in adipose tissue, reinforcing the idea of tapping into this powerful phenomenon in age-related metabolic diseases.

DISCUSSION

A decade of data supports that FGF21 has extensive metabolic benefits in individual tissues, effectively preventing the comorbidities of obesity.[59] Here, we demonstrate that FGF21 overexpression, initiated only in adulthood, extends the lifespan in mice fed a HFD by mechanisms not previously described. Our study illustrates that FGF21, produced selectively in adipocytes, escapes into circulation, and we have confirmed that FGF21 on a HFD in mice exerts endocrine effects through the CNS and peripheral tissues. Consistent with short-term studies using pharmacological administration of FGF21 in adult mice, our transgenic mice exhibited increased energy expenditure and insulin sensitivity in adipose tissue.[6,16] Interestingly, the benefits of FGF21 extended to aged mice, even after its effects on energy expenditure were minimized. Elevated FGF21 throughout the adult life of a mouse fed HFD does not cause growth defects, lower lean mass, or reduce bone density, potential side-effects attributed to sustained FGF21 levels. Elevation of FGF21 in mice fed a HFD prevented weight gain, liver steatosis, and adipose tissue inflammation, metabolic benefits that collectively contributed to increased lifespan. Because FGF21 increases the secretion of the adipokine adiponectin, the extended lifespan of TG mice may rely on heightened adiponectin levels or other factors associated with FGF21 action in adipose tissue. This would be consistent with studies showing that the ablation of adiponectin in mice promotes aging-related diseases and reduces lifespan.[60] This topic is of significant interest, and future studies will address whether adiponectin contributes to FGF21-mediated longevity.

This study illustrates a novel aspect of FGF21's role in systemic metabolism: its regulation of innate and adaptive immunity, particularly in visceral adipose tissue. Importantly, FGF21 protected against alteration in adipose tissue-resident immune activation that reduced inflammation and ceramide synthesis, specifically in visceral fat. Reducing toxic ceramides in adipose and other tissues may significantly drive multi-organ improvements that extend well into late life. We previously[61] identified a critical interaction between FGF21 and adiponectin in the modulation of ceramide levels, especially within scWAT. Our findings are consistent with a model in which adiponectin reduces ceramide levels in adipose tissue. However, in the aged mouse, eWAT has the unique ability to reduce ceramides in response to FGF21, even in the absence of adiponectin. It will be interesting to examine the differences in FGF21 signaling between subcutaneous and visceral fat that drive systemic metabolic improvements.

This evidence strengthens the literature demonstrating that FGF21 signaling confers multiple metabolic benefits through its actions in the CNS and peripheral organs. These benefits include protection against the numerous detrimental impacts of HFD

(C–F) Male ADNKO mice and ADNKO mice with inducible, adipocyte-specific FGF21 expression (ADNKO+TG) fed HFD+dox for 1.5 years. (C and D) Sphingolipid levels in eWAT (C) and scWAT (D) (n = 8). (E and F) Ceramide levels in eWAT (E) and scWAT (F) (n = 8).
$n$number for (A)–(F) denotes biological replicates. Significance in (A)–(F) between control and ADNKO mice or ADNKO and ADNKO+TG mice was calculated using a two-tailed Student's t test. Error bars represent mean ± SEM not significant (ns), $p > 0.05$, $^{*}p < 0.05$, $^{**}p < 0.01$, $^{***}p < 0.001$, and $^{****}p < 0.0001$.

exposure. Given the long-term effectiveness of FGF21 when expressed continuously in mice, it will be exciting to discover if this is achievable in humans. Efforts to increase FGF21 levels, whether pharmacological or inducing endogenous FGF21 with lifestyle changes, could yield significant health benefits, particularly in mitigating obesity-related comorbidities and promoting healthy aging.

FGF21 mediates the stress of overnutrition

As a hormone, FGF21 coordinates metabolic pathways that acclimate to cellular stressors and the subsequent recovery of cell and tissue homeostasis. In healthy organisms on a normal diet, basal circulating FGF21 levels are negligible. Fasting is a canonical stress that increases circulating FGF21, with many studies showing that FGF21 is responsible for many of the benefits of protein-restricted or calorie-restricted diets.[17,62,63] We and others have found that increased tissue expression and serum levels of FGF21 are associated with obesity in mice and humans.[62,64,65] The rise of FGF21 during obesity is not coupled with metabolic benefits but suggests the development of FGF21 signaling resistance.[22] Our data show that adipose tissue-derived FGF21 and/or the elevated circulating levels of FGF21 overcome central or peripheral tissue FGF21 resistance during HFD. Moreover, the overexpression of FGF21 rescued glucose tolerance, insulin sensitivity, and liver steatosis effectively in mice fed a HFD over a lifetime. Our understanding of FGF21 resistance is limited, but our observation is that this resistance can be overcome in mice and may have the potential for effective FGF21 pharmacological treatment in humans.

FGF21 effectively extends lifespan during a HFD challenge

Previous genetic or pharmacological longevity studies manipulating FGF21 were performed in lean mice.[9,17,19,66] Since obesity is a worldwide health problem, we tested whether FGF21 could overcome metabolically unhealthy obesity and its associated comorbidities. We performed the first survival study for FGF21 overexpression induced in mice during adulthood and on a HFD. FGF21 overexpression ameliorated weight gain and many causes of aging-related disease in mice fed a HFD for 1.5 years. FGF21 elevation reduced ectopic lipid deposition in the liver, hyperglycemia, and hyperinsulinemia. Significant improvements in adipose tissue function and insulin sensitivity have broad systemic effects as the adipokine profile shifts. It reduces specific lipid classes that include the ceramides. We have yet to explore all of the benefits of FGF21 during aging. It will be interesting to know which multiorgan role FGF21 has the most significant impact on health and life extension.

FGF21 increases energy expenditure only in young mice fed a HFD

Consistent with previous studies, we observed that FGF21 overexpression stimulated energy expenditure, which contributed to the prevention of weight gain.[16,26] FGF21 has been shown to activate BAT thermogenesis, and it has also been suggested that FGF21 may resensitize BAT or beige adipose tissue to undergo thermogenesis.[67] Notably, the browning/beiging of adipose tissue by FGF21 is temperature and diet-dependent, with brown BAT almost absent in lean mice housed at 30°C or in HFD-fed mice housed at 21°C or 30°C. In our study, adipocyte-specific FGF21 expression in mice fed a HFD for 10 weeks exposed to cold unexpectedly displayed decreased energy expenditure compared with control mice. One possible mechanism is that prolonged FGF21 treatment has been shown to induce energy expenditure, leading to anti-diabetic and anti-obesogenic effects independent of UCP1 and adrenergic signaling.[68,69] Interestingly, FGF21 stimulated locomotor activity in younger mice on a HFD, but this effect was lost in older mice. Undoubtedly, the increased exercise and energy expenditure while the mice were young would contribute to an increased lifespan.

FGF21 immunomodulation in adipose tissue

Accumulation of visceral, but not subcutaneous, adipose tissue is associated with metabolic disease.[70] Visceral fat expansion during aging-obesity is linked to a cascade of inflammation, metabolic dysfunction, and systemic insulin resistance. Dysfunctional adipose tissue promotes the release of cytokines directly from adipocytes or macrophages that infiltrate adipose tissue. We report that adipocyte-specific FGF21 overexpression shifts macrophages toward an anti-inflammatory polarization in mice, lowers B cells, and restores age-related loss of ILC2s to reduce the inflammatory load in VAT.

Notably, β-Klotho is not expressed in macrophages, suggesting that in our study, enhanced FGF21 signaling in adipocytes or other cells that comprise the adipose tissue niche indirectly reduces the burden of macrophages, which may contribute to lowering age-related inflammation. It is evident that FGF21's pleiotropic effects on the visceral fat may lower systemic low-grade inflammation and prevent the development of chronic diseases and degenerative changes during aging.

FGF21 protects against immunological aging of adipose tissue

As demonstrated by Youm et al., FGF21 protects against thymic involution by improving thymic epithelial cell function, which is crucial for maintaining T lymphocyte development.[9,39] We observed that FGF21 overexpression reversed the proportions of $CD8^+$ T cells and Tregs altered by HFD. Although FGF21 does not act directly on peripheral T cells due to the absence of β-Klotho expression in these cells, it has a key role in the thymus, a primary lymphoid organ where T lymphocytes develop. Our data extend these findings by suggesting that either systemic or local FGF21 action in the thymus is protective and might contribute to the reduced inflammatory profile observed in adipose tissue during aging. Others have shown that FGF21 acts as an intrathymic cytokine in the neonatal and juvenile thymus, influencing thymocyte development in a β-Klotho-independent manner.[71] Thus, the intrathymic function of FGF21 may underlie its ability to modulate immune responses and improve systemic metabolism in aged mice, highlighting its potential as a therapeutic target for age-related metabolic and immune dysregulation.

Limitations and future studies

Body weight was lower in the mice with adipose-specific FGF21 overexpression vs. the control group. This occurred early in the study and presents a confounding factor for interpreting which

effects of FGF21 are weight-loss independent. We acknowledge that differences in body weight can complicate the interpretation of metabolic and longevity outcomes. While we did not specifically control for weight differences in these experiments, it is important to note that the metabolic and lifespan effects observed in FGF21-overexpressing mice are consistent with short-term studies described in the previous literature.

Since our mouse model of adipose-specific FGF21 overexpression increases circulating FGF21, it is challenging to distinguish which mechanisms are responsible for systemic, autocrine, or paracrine FGF21 signaling in adipose tissue for the phenotype. While the local effects of FGF21 in adipose and other tissues are recognized as significant, research in this area remains limited.[72] Surprisingly, no publications describe the phenotype of an inducible, adipocyte-specific FGF21 knockout mouse. There is a rationale for developing inducible, tissue-specific mouse models such as β-Klotho and FGFR1c floxed mice in conjunction with FGF21 overexpression, allowing us to tease out the tissue-specific mechanisms of circulating FGF21. Sex-specific effects have been noted for FGF21-mediated metabolic effects in the literature, which we did not address, but we are currently performing these aging studies. Additionally, these models could provide insights into the contribution of local FGF21 to autocrine and paracrine signaling, particularly in relation to its effects on adipocytes, preadipocytes, and immune cells.

Conclusions

Aging and obesity are two of the most significant risk factors for chronic diseases, severely impacting healthspan and lifespan. FGF21 has emerged as a key hormone with the potential to mitigate these risks due to its broad protective effects on metabolic and immune function. Systemic FGF21 has been primarily recognized for its benefits on healthspan and lifespan. However, there is growing evidence that FGF21's beneficial effects may also arise from non-hepatic tissues and involve paracrine or autocrine signaling. In this study, we focused on FGF21's role in adipose tissue, which improved glucose and lipid metabolism and reduced adipose tissue inflammation, particularly under the metabolic stress of a HFD. We identified a unique characteristic of FGF21: reducing harmful ceramide levels, specifically in visceral fat. FGF21's collective actions support overall metabolic resilience, providing a compelling target for therapeutic strategies to prevent or treat type 2 diabetes, cardiovascular disease, and renal disease, i.e., cardiorenal syndrome.

While the development of FGF21 analogs and mimetics is ongoing and provides promise, some limitations exist. FGF21 interventions may require repeated administrations to maintain clinical benefit, which raises concerns about immunological reactions associated with exogenous protein administration.[73,74] Future studies should address whether a systemic increase of FGF21 has the same effects as locally produced FGF21. Visceral adipose tissue-directed FGF21 gene therapy has been tested in mice and could develop into a viable clinical therapeutic.[75] There are several lines of evidence for how humans can increase endogenous FGF21 expression systemically and in specific tissues,[76] such as fasting, which is not an ideal therapeutic option for humans, as it may require a week of fasting.[77] Alternative options to increase FGF21 can be achieved by moderate alcohol consumption,[61] protein restriction,[78] and exercise.[79,80] Our observations demonstrate that FGF21 promotes longevity during a HFD challenge and exerts powerful effects on systemic metabolism through adipose tissue.

RESOURCE AVAILABILITY

Lead contact

Requests for further information and resources should be directed to and will be fulfilled by the lead contact, Philipp E. Scherer (philipp.scherer@UTsouthwestern.edu).

Materials availability

Mice generated in this study will be made available on request, but we may require a payment and/or a completed materials transfer agreement.

Data and code availability

- Data reported in this paper are provided in the supplemental source file or otherwise will be shared by the lead contact upon request.
- This paper does not report original code.
- Any additional information required to reanalyze the data reported in this paper is available from the lead contact upon request.

ACKNOWLEDGMENTS

We thank the UTSW Animal Resource Center, Proteomics Core, Histology Core, Metabolic Phenotyping Core, the Live Cell Imaging Core, Transgenic Core, and Flow Cytometry Facility for their excellent assistance with experiments performed in this paper. We also thank Shimadzu Scientific Instruments for the collaborative efforts in mass spectrometry technology resources and Dr. David Mangelsdorf and Dr. Steven Kliewer at UTSW for providing valuable conversations and insights on this work. We thank Charlotte E. Lee for her invaluable contributions and expertise in histological techniques. This study was supported by US NIH grant 5P01AG051459-08 to V.D.D, T.L.H., and P.E.S.; US NIH grants RC2-DK118620, R01-DK55758, R01-DK099110, R01-DK127274, and R01-DK131537 to P.E.S.; US NIH grant K01-DK131252 to C.M.G.; US NIH grants R00-AG068239, R01-AG084646, and R01-DK138038 and the Hevolution Foundation (HF-GRO-23-1199262-27) to S.Z.; US NIH grants 5P01AG051459-08, 5U54AG079759-03, and 5R01AG068863-05 to V.D.D.; US NIH grants 5R01DK136619-02 and 1R01DK136532-01 to Y.Z.; and US NIH grants R01-DK114036 and R00-DK122019 to C.C.

AUTHOR CONTRIBUTIONS

Conceptualization, P.E.S. and V.D.D.; methodology, P.E.S., Z.Z., Y.Z., S.Z., Y.-H.Y., and C.M.G.; investigation, C.M.G., R.G., Y.-H.Y., Q.L., C.C., M.V., S.Z., Y.Z., T.F., B.F., and C.J.R.; writing – original draft, C.M.G.; writing – review and editing, C.M.G., P.E.S., and V.D.D.; funding acquisition, P.E.S., T.L.H., and V.D.D.; resources, P.E.S., T.L.H., and V.D.D.; supervision, P.E.S. and V.D.D.

DECLARATION OF INTERESTS

The authors declare no competing interests.

STAR★METHODS

Detailed methods are provided in the online version of this paper and include the following:

- KEY RESOURCES TABLE
- EXPERIMENTAL MODEL AND STUDY PARTICIPANT DETAILS
  - Mouse models
- METHOD DETAILS
  - Body composition analysis
  - Oral glucose tolerance test
  - Insulin tolerance test
  - Beta-3 adrenergic receptor agonist test

SUPPLEMENTAL INFORMATION

Supplemental information can be found online at https://doi.org/10.1016/j.cmet.2025.05.011.

Received: November 26, 2024
Revised: February 27, 2025
Accepted: May 19, 2025
Published: June 16, 2025

REFERENCES

1. Fakhouri, T.H.I., Ogden, C.L., Carroll, M.D., Kit, B.K., and Flegal, K.M. (2012). Prevalence of obesity among older adults in the United States, 2007–2010. NCHS Data Brief *106*, 1–8.
2. Goldberg, E.L., and Dixit, V.D. (2015). Drivers of age-related inflammation and strategies for healthspan extension. Immunol. Rev. *265*, 63–74. https://doi.org/10.1111/imr.12295.
3. Markan, K.R., Naber, M.C., Ameka, M.K., Anderegg, M.D., Mangelsdorf, D.J., Kliewer, S.A., Mohammadi, M., and Potthoff, M.J. (2014). Circulating FGF21 is liver derived and enhances glucose uptake during refeeding and overfeeding. Diabetes *63*, 4057–4063. https://doi.org/10.2337/db14-0595.
4. Fisher, F.M., and Maratos-Flier, E. (2016). Understanding the Physiology of FGF21. Annu. Rev. Physiol. *78*, 223–241. https://doi.org/10.1146/annurev-physiol-021115-105339.
5. Kharitonenkov, A., Wroblewski, V.J., Koester, A., Chen, Y.F., Clutinger, C.K., Tigno, X.T., Hansen, B.C., Shanafelt, A.B., and Etgen, G.J. (2007). The metabolic state of diabetic monkeys is regulated by fibroblast growth factor-21. Endocrinology *148*, 774–781. https://doi.org/10.1210/en.2006-1168.
6. Talukdar, S., Zhou, Y., Li, D., Rossulek, M., Dong, J., Somayaji, V., Weng, Y., Clark, R., Lanba, A., Owen, B.M., et al. (2016). A Long-Acting FGF21 Molecule, PF-05231023, Decreases Body Weight and Improves Lipid Profile in Non-human Primates and Type 2 Diabetic Subjects. Cell Metab. *23*, 427–440. https://doi.org/10.1016/j.cmet.2016.02.001.
7. Adams, A.C., Halstead, C.A., Hansen, B.C., Irizarry, A.R., Martin, J.A., Myers, S.R., Reynolds, V.L., Smith, H.W., Wroblewski, V.J., and Kharitonenkov, A. (2013). LY2405319, an Engineered FGF21 Variant, Improves the Metabolic Status of Diabetic Monkeys. PLoS One *8*, e65763. https://doi.org/10.1371/journal.pone.0065763.
8. Jimenez, V., Jambrina, C., Casana, E., Sacristan, V., Munoz, S., Darriba, S., Rodo, J., Mallol, C., Garcia, M., Leon, X., et al. (2018). FGF21 gene therapy as treatment for obesity and insulin resistance. EMBO Mol. Med. *10*, e8791. https://doi.org/10.15252/emmm.201708791.
9. Youm, Y.H., Horvath, T.L., Mangelsdorf, D.J., Kliewer, S.A., and Dixit, V.D. (2016). Prolongevity hormone FGF21 protects against immune senescence by delaying age-related thymic involution. Proc. Natl. Acad. Sci. USA *113*, 1026–1031. https://doi.org/10.1073/pnas.1514511113.
10. Fisher, F.M., Kleiner, S., Douris, N., Fox, E.C., Mepani, R.J., Verdeguer, F., Wu, J., Kharitonenkov, A., Flier, J.S., Maratos-Flier, E., et al. (2012). FGF21 regulates PGC-1alpha and browning of white adipose tissues in adaptive thermogenesis. Genes Dev. *26*, 271–281. https://doi.org/10.1101/gad.177857.111.
11. Arias-Calderon, M., Casas, M., Balanta-Melo, J., Morales-Jimenez, C., Hernandez, N., Llanos, P., Jaimovich, E., and Buvinic, S. (2023). Fibroblast growth factor 21 is expressed and secreted from skeletal muscle following electrical stimulation via extracellular ATP activation of the PI3K/Akt/mTOR signaling pathway. Front. Endocrinol. (Lausanne) *14*, 1059020. https://doi.org/10.3389/fendo.2023.1059020.
12. Coate, K.C., Hernandez, G., Thorne, C.A., Sun, S., Le, T.D.V., Vale, K., Kliewer, S.A., and Mangelsdorf, D.J. (2017). FGF21 Is an Exocrine Pancreas Secretagogue. Cell Metab. *25*, 472–480. https://doi.org/10.1016/j.cmet.2016.12.004.
13. Adams, A.C., Cheng, C.C., Coskun, T., and Kharitonenkov, A. (2012). FGF21 requires betaklotho to act in vivo. PLoS One *7*, e49977. https://doi.org/10.1371/journal.pone.0049977.
14. Adams, A.C., Yang, C., Coskun, T., Cheng, C.C., Gimeno, R.E., Luo, Y., and Kharitonenkov, A. (2012). The breadth of FGF21's metabolic actions are governed by FGFR1 in adipose tissue. Mol. Metab. *2*, 31–37. https://doi.org/10.1016/j.molmet.2012.08.007.
15. Geng, L., Lam, K.S.L., and Xu, A. (2020). The therapeutic potential of FGF21 in metabolic diseases: from bench to clinic. Nat. Rev. Endocrinol. *16*, 654–667. https://doi.org/10.1038/s41574-020-0386-0.
16. BonDurant, L.D., Ameka, M., Naber, M.C., Markan, K.R., Idiga, S.O., Acevedo, M.R., Walsh, S.A., Ornitz, D.M., and Potthoff, M.J. (2017). FGF21 Regulates Metabolism Through Adipose-Dependent and -Independent Mechanisms. Cell Metab. *25*, 935–944.e4. https://doi.org/10.1016/j.cmet.2017.03.005.
17. Hill, C.M., Albarado, D.C., Coco, L.G., Spann, R.A., Khan, M.S., Qualls-Creekmore, E., Burk, D.H., Burke, S.J., Collier, J.J., Yu, S., et al. (2022). FGF21 is required for protein restriction to extend lifespan and improve metabolic health in male mice. Nat. Commun. *13*, 1897. https://doi.org/10.1038/s41467-022-29499-8.
18. Inagaki, T., Lin, V.Y., Goetz, R., Mohammadi, M., Mangelsdorf, D.J., and Kliewer, S.A. (2008). Inhibition of growth hormone signaling by the fasting-induced hormone FGF21. Cell Metab. *8*, 77–83. https://doi.org/10.1016/j.cmet.2008.05.006.
19. Zhang, Y., Xie, Y., Berglund, E.D., Coate, K.C., He, T.T., Katafuchi, T., Xiao, G., Potthoff, M.J., Wei, W., Wan, Y., et al. (2012). The starvation hormone, fibroblast growth factor-21, extends lifespan in mice. eLife *1*, e00065. https://doi.org/10.7554/eLife.00065.
20. Fazeli, P.K., Lun, M., Kim, S.M., Bredella, M.A., Wright, S., Zhang, Y., Lee, H., Catana, C., Klibanski, A., Patwari, P., et al. (2015). FGF21 and the late adaptive response to starvation in humans. J. Clin. Invest. *125*, 4601–4611. https://doi.org/10.1172/JCI83349.
21. Nygaard, E.B., Moller, C.L., Kievit, P., Grove, K.L., and Andersen, B. (2014). Increased fibroblast growth factor 21 expression in high-fat diet-sensitive non-human primates (Macaca mulatta). Int. J. Obes. (Lond.) *38*, 183–191. https://doi.org/10.1038/ijo.2013.79.
22. Fisher, F.M., Chui, P.C., Antonellis, P.J., Bina, H.A., Kharitonenkov, A., Flier, J.S., and Maratos-Flier, E. (2010). Obesity is a fibroblast growth factor 21 (FGF21)-resistant state. Diabetes *59*, 2781–2789. https://doi.org/10.2337/db10-0193.
23. Potthoff, M.J., Inagaki, T., Satapati, S., Ding, X., He, T., Goetz, R., Mohammadi, M., Finck, B.N., Mangelsdorf, D.J., Kliewer, S.A., et al. (2009). FGF21 induces PGC-1alpha and regulates carbohydrate and fatty acid metabolism during the adaptive starvation response. Proc. Natl. Acad. Sci. USA. *106*, 10853–10858. https://doi.org/10.1073/pnas.0904187106.
24. Hill, C.M., Laeger, T., Dehner, M., Albarado, D.C., Clarke, B., Wanders, D., Burke, S.J., Collier, J.J., Qualls-Creekmore, E., Solon-Biet, S.M., et al. (2019). FGF21 Signals Protein Status to the Brain and Adaptively Regulates Food Choice and Metabolism. Cell Rep. *27*, 2934–2947.e3. https://doi.org/10.1016/j.celrep.2019.05.022.
25. Solon-Biet, S.M., Clark, X., Bell-Anderson, K., Rusu, P.M., Perks, R., Freire, T., Pulpitel, T., Senior, A.M., Hoy, A.J., Aung, O., et al. (2023). Toward reconciling the roles of FGF21 in protein appetite, sweet preference, and energy expenditure. Cell Rep. *42*, 113536. https://doi.org/10.1016/j.celrep.2023.113536.
26. Owen, B.M., Ding, X., Morgan, D.A., Coate, K.C., Bookout, A.L., Rahmouni, K., Kliewer, S.A., and Mangelsdorf, D.J. (2014). FGF21 acts centrally to induce sympathetic nerve activity, energy expenditure, and weight loss. Cell Metab. *20*, 670–677. https://doi.org/10.1016/j.cmet.2014.07.012.

27. Charoenphandhu, N., Suntornsaratoon, P., Krishnamra, N., Sa-Nguanmoo, P., Tanajak, P., Wang, X., Liang, G., Li, X., Jiang, C., Chattipakorn, N., et al. (2017). Fibroblast growth factor-21 restores insulin sensitivity but induces aberrant bone microstructure in obese insulin-resistant rats. J. Bone Miner. Metab. *35*, 142–149. https://doi.org/10.1007/s00774-016-0745-z.

28. Hao, R.H., Gao, J.L., Li, M., Huang, W., Zhu, D.L., Thynn, H.N., Dong, S.S., and Guo, Y. (2018). Association between fibroblast growth factor 21 and bone mineral density in adults. Endocrine *59*, 296–303. https://doi.org/10.1007/s12020-017-1507-y.

29. Wei, W., Dutchak, P.A., Wang, X., Ding, X., Wang, X., Bookout, A.L., Goetz, R., Mohammadi, M., Gerard, R.D., Dechow, P.C., et al. (2012). Fibroblast growth factor 21 promotes bone loss by potentiating the effects of peroxisome proliferator-activated receptor gamma. Proc. Natl. Acad. Sci. USA. *109*, 3143–3148. https://doi.org/10.1073/pnas.1200797109.

30. Mina, A.I., LeClair, R.A., LeClair, K.B., Cohen, D.E., Lantier, L., and Banks, A.S. (2018). CalR: A Web-Based Analysis Tool for Indirect Calorimetry Experiments. Cell Metab. *28*, 656–666.e1. https://doi.org/10.1016/j.cmet.2018.06.019.

31. Liu, C., Schonke, M., Spoorenberg, B., Lambooij, J.M., van der Zande, H. J.P., Zhou, E., Tushuizen, M.E., Andreasson, A.C., Park, A., Oldham, S., et al. (2023). FGF21 protects against hepatic lipotoxicity and macrophage activation to attenuate fibrogenesis in nonalcoholic steatohepatitis. eLife *12*, e83075. https://doi.org/10.7554/eLife.83075.

32. Zhang, J., Gupte, J., Gong, Y., Weiszmann, J., Zhang, Y., Lee, K.J., Richards, W.G., and Li, Y. (2017). Chronic Over-expression of Fibroblast Growth Factor 21 Increases Bile Acid Biosynthesis by Opposing FGF15/19 Action. EBioMedicine *15*, 173–183. https://doi.org/10.1016/j.ebiom.2016.12.016.

33. Schlein, C., Talukdar, S., Heine, M., Fischer, A.W., Krott, L.M., Nilsson, S. K., Brenner, M.B., Heeren, J., and Scheja, L. (2016). FGF21 Lowers Plasma Triglycerides by Accelerating Lipoprotein Catabolism in White and Brown Adipose Tissues. Cell Metab. *23*, 441–453. https://doi.org/10.1016/j.cmet.2016.01.006.

34. Lee, A.H., and Dixit, V.D. (2020). Dietary Regulation of Immunity. Immunity *53*, 510–523. https://doi.org/10.1016/j.immuni.2020.08.013.

35. Lumeng, C.N., Bodzin, J.L., and Saltiel, A.R. (2007). Obesity induces a phenotypic switch in adipose tissue macrophage polarization. J. Clin. Invest. *117*, 175–184. https://doi.org/10.1172/JCI29881.

36. Weisberg, S.P., McCann, D., Desai, M., Rosenbaum, M., Leibel, R.L., and Ferrante, A.W., Jr. (2003). Obesity is associated with macrophage accumulation in adipose tissue. J. Clin. Invest. *112*, 1796–1808. https://doi.org/10.1172/JCI19246.

37. Hotamisligil, G.S., Shargill, N.S., and Spiegelman, B.M. (1993). Adipose expression of tumor necrosis factor-alpha: direct role in obesity-linked insulin resistance. Science *259*, 87–91. https://doi.org/10.1126/science.7678183.

38. Camell, C.D., Gunther, P., Lee, A., Goldberg, E.L., Spadaro, O., Youm, Y. H., Bartke, A., Hubbard, G.B., Ikeno, Y., Ruddle, N.H., et al. (2019). Aging Induces an Nlrp3 Inflammasome-Dependent Expansion of Adipose B Cells That Impairs Metabolic Homeostasis. Cell Metab. *30*, 1024–1039.e6. https://doi.org/10.1016/j.cmet.2019.10.006.

39. Youm, Y.H., Gliniak, C., Zhang, Y., Dlugos, T., Scherer, P.E., and Dixit, V. D. (2025). Enhanced paracrine action of FGF21 in stromal cells delays thymic aging. Nat Aging *5*, 576–587. https://doi.org/10.1038/s43587-025-00813-5.

40. Mehta, P., Nuotio-Antar, A.M., and Smith, C.W. (2015). gammadelta T cells promote inflammation and insulin resistance during high fat diet-induced obesity in mice. J. Leukoc. Biol. *97*, 121–134. https://doi.org/10.1189/jlb.3A0414-211RR.

41. Muñoz-Rojas, A.R., Wang, G., Benoist, C., and Mathis, D. (2024). Adipose-tissue regulatory T cells are a consortium of subtypes that evolves with age and diet. Proc. Natl. Acad. Sci. USA *121*, e2320602121. https://doi.org/10.1073/pnas.2320602121.

42. Kohlgruber, A.C., Gal-Oz, S.T., LaMarche, N.M., Shimazaki, M., Duquette, D., Koay, H.F., Nguyen, H.N., Mina, A.I., Paras, T., Tavakkoli, A., et al. (2018). gammadelta T cells producing interleukin-17A regulate adipose regulatory T cell homeostasis and thermogenesis. Nat. Immunol. *19*, 464–474. https://doi.org/10.1038/s41590-018-0094-2.

43. Bapat, S.P., Myoung Suh, J., Fang, S., Liu, S., Zhang, Y., Cheng, A., Zhou, C., Liang, Y., LeBlanc, M., Liddle, C., et al. (2015). Depletion of fat-resident Treg cells prevents age-associated insulin resistance. Nature *528*, 137–141. https://doi.org/10.1038/nature16151.

44. Badman, M.K., Pissios, P., Kennedy, A.R., Koukos, G., Flier, J.S., and Maratos-Flier, E. (2007). Hepatic fibroblast growth factor 21 is regulated by PPARalpha and is a key mediator of hepatic lipid metabolism in ketotic states. Cell Metab. *5*, 426–437. https://doi.org/10.1016/j.cmet.2007.05.002.

45. Feuerer, M., Herrero, L., Cipolletta, D., Naaz, A., Wong, J., Nayer, A., Lee, J., Goldfine, A.B., Benoist, C., Shoelson, S., et al. (2009). Lean, but not obese, fat is enriched for a unique population of regulatory T cells that affect metabolic parameters. Nat. Med. *15*, 930–939. https://doi.org/10.1038/nm.2002.

46. Goldberg, E.L., Shchukina, I., Youm, Y.H., Ryu, S., Tsusaka, T., Young, K. C., Camell, C.D., Dlugos, T., Artyomov, M.N., and Dixit, V.D. (2021). IL-33 causes thermogenic failure in aging by expanding dysfunctional adipose ILC2. Cell Metab. *33*, 2277–2287.e5. https://doi.org/10.1016/j.cmet.2021.08.004.

47. Holland, W.L., Adams, A.C., Brozinick, J.T., Bui, H.H., Miyauchi, Y., Kusminski, C.M., Bauer, S.M., Wade, M., Singhal, E., Cheng, C.C., et al. (2013). An FGF21-adiponectin-ceramide axis controls energy expenditure and insulin action in mice. Cell Metab. *17*, 790–797. https://doi.org/10.1016/j.cmet.2013.03.019.

48. Turpin, S.M., Nicholls, H.T., Willmes, D.M., Mourier, A., Brodesser, S., Wunderlich, C.M., Mauer, J., Xu, E., Hammerschmidt, P., Bronneke, H. S., et al. (2014). Obesity-induced CerS6-dependent C16:0 ceramide production promotes weight gain and glucose intolerance. Cell Metab. *20*, 678–686. https://doi.org/10.1016/j.cmet.2014.08.002.

49. Choi, R.H., Tatum, S.M., Symons, J.D., Summers, S.A., and Holland, W.L. (2021). Ceramides and other sphingolipids as drivers of cardiovascular disease. Nat. Rev. Cardiol. *18*, 701–711. https://doi.org/10.1038/s41569-021-00536-1.

50. Holland, W.L., Miller, R.A., Wang, Z.V., Sun, K., Barth, B.M., Bui, H.H., Davis, K.E., Bikman, B.T., Halberg, N., Rutkowski, J.M., et al. (2011). Receptor-mediated activation of ceramidase activity initiates the pleiotropic actions of adiponectin. Nat. Med. *17*, 55–63. https://doi.org/10.1038/nm.2277.

51. Hernandez-Corbacho, M.J., Jenkins, R.W., Clarke, C.J., Hannun, Y.A., Obeid, L.M., Snider, A.J., and Siskind, L.J. (2011). Accumulation of long-chain glycosphingolipids during aging is prevented by caloric restriction. PLoS One *6*, e20411. https://doi.org/10.1371/journal.pone.0020411.

52. Novgorodov, S.A., Riley, C.L., Yu, J., Keffler, J.A., Clarke, C.J., Van Laer, A.O., Baicu, C.F., Zile, M.R., and Gudz, T.I. (2016). Lactosylceramide contributes to mitochondrial dysfunction in diabetes. J. Lipid Res. *57*, 546–562. https://doi.org/10.1194/jlr.M060061.

53. Shu, H., Peng, Y., Hang, W., Li, N., Zhou, N., and Wang, D.W. (2022). Emerging Roles of Ceramide in Cardiovascular Diseases. Aging Dis. *13*, 232–245. https://doi.org/10.14336/AD.2021.0710.

54. Kotronen, A., Seppanen-Laakso, T., Westerbacka, J., Kiviluoto, T., Arola, J., Ruskeepaa, A.L., Yki-Jarvinen, H., and Oresic, M. (2010). Comparison of lipid and fatty acid composition of the liver, subcutaneous and intra-abdominal adipose tissue, and serum. Obesity (Silver Spring) *18*, 937–944. https://doi.org/10.1038/oby.2009.326.

55. Vandanmagsar, B., Youm, Y.H., Ravussin, A., Galgani, J.E., Stadler, K., Mynatt, R.L., Ravussin, E., Stephens, J.M., and Dixit, V.D. (2011). The NLRP3 inflammasome instigates obesity-induced inflammation and insulin resistance. Nat. Med. *17*, 179–188. https://doi.org/10.1038/nm.2279.

56. Youm, Y.H., Kanneganti, T.D., Vandanmagsar, B., Zhu, X., Ravussin, A., Adijiang, A., Owen, J.S., Thomas, M.J., Francis, J., Parks, J.S., et al.

(2012). The Nlrp3 inflammasome promotes age-related thymic demise and immunosenescence. Cell Rep. *1*, 56–68. https://doi.org/10.1016/j.celrep.2011.11.005.

57. Smith, A.B., Schill, J.P., Gordillo, R., Gustafson, G.E., Rhoads, T.W., Burhans, M.S., Broman, A.T., Colman, R.J., Scherer, P.E., and Anderson, R.M. (2022). Ceramides are early responders in metabolic syndrome development in rhesus monkeys. Sci. Rep. *12*, 9960. https://doi.org/10.1038/s41598-022-14083-3.

58. Nawrocki, A.R., Rajala, M.W., Tomas, E., Pajvani, U.B., Saha, A.K., Trumbauer, M.E., Pang, Z., Chen, A.S., Ruderman, N.B., Chen, H., et al. (2006). Mice lacking adiponectin show decreased hepatic insulin sensitivity and reduced responsiveness to peroxisome proliferator-activated receptor gamma agonists. J. Biol. Chem. *281*, 2654–2660. https://doi.org/10.1074/jbc.M505311200.

59. Kliewer, S.A., and Mangelsdorf, D.J. (2019). A Dozen Years of Discovery: Insights into the Physiology and Pharmacology of FGF21. Cell Metab. *29*, 246–253. https://doi.org/10.1016/j.cmet.2019.01.004.

60. Li, N., Zhao, S., Zhang, Z., Zhu, Y., Gliniak, C.M., Vishvanath, L., An, Y.A., Wang, M.Y., Deng, Y., Zhu, Q., et al. (2021). Adiponectin preserves metabolic fitness during aging. eLife *10*, e65108. https://doi.org/10.7554/eLife.65108.

61. Song, P., Zechner, C., Hernandez, G., Cánovas, J., Xie, Y., Sondhi, V., Wagner, M., Stadlbauer, V., Horvath, A., Leber, B., et al. (2018). The Hormone FGF21 Stimulates Water Drinking in Response to Ketogenic Diet and Alcohol. Cell Metab. *27*, 1338–1347.e4. https://doi.org/10.1016/j.cmet.2018.04.001.

62. Badman, M.K., Kennedy, A.R., Adams, A.C., Pissios, P., and Maratos-Flier, E. (2009). A very low carbohydrate ketogenic diet improves glucose tolerance in ob/ob mice independently of weight loss. Am. J. Physiol. Endocrinol. Metab. *297*, E1197–E1204. https://doi.org/10.1152/ajpendo.00357.2009.

63. Wanders, D., Forney, L.A., Stone, K.P., Burk, D.H., Pierse, A., and Gettys, T.W. (2017). FGF21 Mediates the Thermogenic and Insulin-Sensitizing Effects of Dietary Methionine Restriction but Not Its Effects on Hepatic Lipid Metabolism. Diabetes *66*, 858–867. https://doi.org/10.2337/db16-1212.

64. Zhang, X., Yeung, D.C.Y., Karpisek, M., Stejskal, D., Zhou, Z.G., Liu, F., Wong, R.L.C., Chow, W.S., Tso, A.W.K., Lam, K.S.L., et al. (2008). Serum FGF21 levels are increased in obesity and are independently associated with the metabolic syndrome in humans. Diabetes *57*, 1246–1253. https://doi.org/10.2337/db07-1476.

65. Dushay, J., Chui, P.C., Gopalakrishnan, G.S., Varela-Rey, M., Crawley, M., Fisher, F.M., Badman, M.K., Martinez-Chantar, M.L., and Maratos-Flier, E. (2010). Increased fibroblast growth factor 21 in obesity and nonalcoholic fatty liver disease. Gastroenterology *139*, 456–463. https://doi.org/10.1053/j.gastro.2010.04.054.

66. Anderson, J.M., Arnold, W.D., Huang, W., Ray, A., Owendoff, G., and Cao, L. (2024). Long-term effects of a fat-directed FGF21 gene therapy in aged female mice. Gene Ther. *31*, 95–104. https://doi.org/10.1038/s41434-023-00422-0.

67. Ameka, M., Markan, K.R., Morgan, D.A., BonDurant, L.D., Idiga, S.O., Naber, M.C., Zhu, Z., Zingman, L.V., Grobe, J.L., Rahmouni, K., et al. (2019). Liver Derived FGF21 Maintains Core Body Temperature During Acute Cold Exposure. Sci. Rep. *9*, 630. https://doi.org/10.1038/s41598-018-37198-y.

68. Véniant, M.M., Sivits, G., Helmering, J., Komorowski, R., Lee, J., Fan, W., Moyer, C., and Lloyd, D.J. (2015). Pharmacologic Effects of FGF21 Are Independent of the "Browning" of White Adipose Tissue. Cell Metab. *21*, 731–738. https://doi.org/10.1016/j.cmet.2015.04.019.

69. Stanic, S., Bardova, K., Janovska, P., Rossmeisl, M., Kopecky, J., and Zouhar, P. (2024). Prolonged FGF21 treatment increases energy expenditure and induces weight loss in obese mice independently of UCP1 and adrenergic signaling. Biochem. Pharmacol. *221*, 116042. https://doi.org/10.1016/j.bcp.2024.116042.

70. Klein, S., Allison, D.B., Heymsfield, S.B., Kelley, D.E., Leibel, R.L., Nonas, C., and Kahn, R. (2007). Waist circumference and cardiometabolic risk: a consensus statement from shaping America's health, the Association for Weight Management and Obesity Prevention; NAASO, the Obesity Society; the American Society for Nutrition; and the American Diabetes Association. Diabetes Care *30*, 1647–1652. https://doi.org/10.2337/dc07-9921.

71. Nakayama, Y., Masuda, Y., Ohta, H., Tanaka, T., Washida, M., Nabeshima, Y.I., Miyake, A., Itoh, N., and Konishi, M. (2017). Fgf21 regulates T-cell development in the neonatal and juvenile thymus. Sci. Rep. *7*, 330. https://doi.org/10.1038/s41598-017-00349-8.

72. Spann, R.A., Morrison, C.D., and den Hartigh, L.J. (2021). The Nuanced Metabolic Functions of Endogenous FGF21 Depend on the Nature of the Stimulus, Tissue Source, and Experimental Model. Front. Endocrinol. (Lausanne) *12*, 802541. https://doi.org/10.3389/fendo.2021.802541.

73. Gaich, G., Chien, J.Y., Fu, H., Glass, L.C., Deeg, M.A., Holland, W.L., Kharitonenkov, A., Bumol, T., Schilske, H.K., and Moller, D.E. (2013). The effects of LY2405319, an FGF21 analog, in obese human subjects with type 2 diabetes. Cell Metab. *18*, 333–340. https://doi.org/10.1016/j.cmet.2013.08.005.

74. Charles, E.D., Neuschwander-Tetri, B.A., Pablo Frias, J., Kundu, S., Luo, Y., Tirucherai, G.S., and Christian, R. (2019). Pegbelfermin (BMS-986036), PEGylated FGF21, in Patients with Obesity and Type 2 Diabetes: Results from a Randomized Phase 2 Study. Obesity (Silver Spring) *27*, 41–49. https://doi.org/10.1002/oby.22344.

75. Queen, N.J., Bates, R., Huang, W., Xiao, R., Appana, B., and Cao, L. (2021). Visceral adipose tissue-directed FGF21 gene therapy improves metabolic and immune health in BTBR mice. Mol. Ther. Methods Clin. Dev. *20*, 409–422. https://doi.org/10.1016/j.omtm.2020.12.011.

76. Qian, Z., Zhang, Y., Yang, N., Nie, H., Yang, Z., Luo, P., Wei, X., Guan, Y., Huang, Y., Yan, J., et al. (2022). Close association between lifestyle and circulating FGF21 levels: A systematic review and meta-analysis. Front. Endocrinol. (Lausanne) *13*, 984828. https://doi.org/10.3389/fendo.2022.984828.

77. Galman, C., Lundasen, T., Kharitonenkov, A., Bina, H.A., Eriksson, M., Hafstrom, I., Dahlin, M., Amark, P., Angelin, B., and Rudling, M. (2008). The circulating metabolic regulator FGF21 is induced by prolonged fasting and PPARalpha activation in man. Cell Metab. *8*, 169–174. https://doi.org/10.1016/j.cmet.2008.06.014.

78. Laeger, T., Henagan, T.M., Albarado, D.C., Redman, L.M., Bray, G.A., Noland, R.C., Münzberg, H., Hutson, S.M., Gettys, T.W., Schwartz, M.W., et al. (2014). FGF21 is an endocrine signal of protein restriction. J. Clin. Invest. *124*, 3913–3922. https://doi.org/10.1172/JCI74915.

79. Geng, L., Liao, B., Jin, L., Huang, Z., Triggle, C.R., Ding, H., Zhang, J., Huang, Y., Lin, Z., and Xu, A. (2019). Exercise Alleviates Obesity-Induced Metabolic Dysfunction via Enhancing FGF21 Sensitivity in Adipose Tissues. Cell Rep. *26*, 2738–2752.e4. https://doi.org/10.1016/j.celrep.2019.02.014.

80. Cuevas-Ramos, D., Almeda-Valdes, P., Meza-Arana, C.E., Brito-Cordova, G., Gomez-Perez, F.J., Mehta, R., Oseguera-Moguel, J., and Aguilar-Salinas, C.A. (2012). Exercise increases serum fibroblast growth factor 21 (FGF21) levels. PLoS One *7*, e38022. https://doi.org/10.1371/journal.pone.0038022.

81. Wang, X., and Seed, B. (2003). A PCR primer bank for quantitative gene expression analysis. Nucleic Acids Res. *31*, e154. https://doi.org/10.1093/nar/gng154.

82. Livak, K.J., and Schmittgen, T.D. (2001). Analysis of relative gene expression data using real-time quantitative PCR and the 2(-Delta Delta C(T)) Method. Methods *25*, 402–408. https://doi.org/10.1006/meth.2001.1262.

83. Cannavino, J., Shao, M., An, Y.A., Bezprozvannaya, S., Chen, S., Kim, J., Xu, L., McAnally, J.R., Scherer, P.E., Liu, N., et al. (2021). Regulation of cold-induced thermogenesis by the RNA binding protein FAM195A. Proc. Natl. Acad. Sci. USA *118*, e2104650118. https://doi.org/10.1073/pnas.2104650118.

STAR★METHODS

KEY RESOURCES TABLE

REAGENT or RESOURCE	SOURCE	IDENTIFIER
Antibodies		
Anti-FGF21	BioVendor	Cat# RD291108200R; RRID: AB_2909467
Anti-AKT	Cell Signaling Technology	Cat# 9272; RRID: AB_329827
Anti-pAKT (S473)	Cell Signaling Technology	Cat# 9271; RRID: AB_329825
Anti-β-actin	Sigma-Aldrich	Cat# A5441; RRID: AB_476744
Anti-ERK	Cell Signaling Technology	Cat# 9102; RRID: AB_330744
Anti-pERK (T202/Y204)	Cell Signaling Technology	Cat# 4370; RRID: AB_2315112
IRDye® 800CW Goat anti-Rabbit IgG Secondary Antibody	LI-COR Biosciences	Cat# 926-32211; RRID: AB_621843
IRDye® 680RD Donkey anti-Mouse IgG Secondary Antibody	LI-COR Biosciences	Cat# 926-68072; RRID: AB_10953628
FcBlock CD16/32	Thermo Fisher Scientific	Cat# 14-0161-82; RRID: AB_467133
Live/Dead viability dye (Aqua)	Thermo Fisher Scientific	Cat# L34966
CD45 (BV711), CD45 (APC)	Biolegend Thermo Fisher Scientific	Cat# 103147; RRID: AB_2564383, Cat# 17-0451-83; RRID: AB_469393
CD25	Biolegend	Cat# 102035; RRID: AB_11126977
CD127	Biolegend	Cat# 135012; RRID: AB_1937216
ST2 (IL1RL1)	Thermo Fisher Scientific	Cat# 25-9335-82; RRID: AB_2637464
CD3	Biolegend	Cat# 100216; RRID: AB_493697
TCRb	Biolegend	Cat# 109224; RRID: AB_1027648
CD11b (PerCP-Cy5.5) CD11b (BV711)	Thermo Fisher Scientific, Biolegend	Cat# 56-0112-82; RRID: AB_657585, Cat# 101241; RRID: AB_11218791
B220/CD45R	Thermo Fisher Scientific	Cat# 17-0452-83; RRID: AB_469396
CD11c (AF700), CD11c (PE-Cy7)	Biolegend	Cat# 117320; RRID: AB_528736, Cat# 117317; RRID: AB_493569
F4/80	Biolegend	Cat# 123130; RRID: AB_2293450
Gr1 (Ly-6G)	Biolegend	Cat# 127622; RRID: AB_10643269
FCeRIα	Biolegend	Cat# 134324; RRID: AB_2566734
Ter119	Biolegend	Cat# 116220; RRID: AB_528963
CD5	Biolegend	Cat# 100636; RRID: AB_2687002
CD19	Biolegend	Cat# 115528; RRID: AB_493735
CD21	Thermo Fisher Scientific	Cat# 12-0212-82; RRID: AB_10870784
CD23	Thermo Fisher Scientific	Cat# 48-0232-82; RRID: AB_11220067
CD44	BD	Cat# 741471; RRID: AB_2870939
FoxP3 (Intracellular)	Thermo Fisher Scientific	Cat# 25-5773-82; RRID: AB_891552
CD206 (AF488), CD206 (APC780)	Biolegend, Thermo Fisher Scientific	Cat# 141710; RRID: AB_10900445, Cat# 47-2061-82; RRID: AB_2802285
CD4 (BV605). CD4 (BV615)	Biolegend, BD	Cat# 100451; RRID: AB_2564591, Cat# 613006; RRID: AB_2870274
CD8	Biolegend	Cat# 612898; RRID: AB_2870186
NK1.1	Biolegend	Cat# 108730; RRID: AB_2291262
TCRgd	Biolegend	Cat# 118108; RRID: AB_313832
Biological samples		
Serum samples (mouse)	This paper	N/A
Adipose, liver, and blood tissues (mouse)	This paper	N/A

(*Continued on next page*)

Continued

REAGENT or RESOURCE	SOURCE	IDENTIFIER
Chemicals, peptides, and recombinant proteins		
Dextrose	Thermo Fisher Scientific	Cat# D16-500
Hank's Balanced Salt Solution	Life Technologies	Cat# 14175095
Collagenase II	Worthington Biochemicals	Cat# LS004176
ACK lysis buffer	Quality Biological	Cat# 118-156-101
RPMI-1640	Thermo Fisher Scientific	Cat# FB12999107
Fetal Bovine Serum	Thermo Fisher Scientific	Cat# FB12999102
NuPAGE 4%–12% Bis-Tris Gel	Thermo Fisher Scientific	Cat# NP0335BOX
CL 316,243	Sigma-Aldrich	Cat# C5976
iScript cDNA Synthesis Kit	BIORAD	Cat# 1708890
Trizol reagent	Invitrogen	Cat# 15596018
PowerUp SYBR Green Master Mix	Thermo Fisher Scientific	Cat# A25741
Cell Lysis Buffer	Cell Signaling Technology	Cat# 9803
Halt Protease and Phosphatase Inhibitor	Thermo Fisher Scientific	Cat# 78442
BCA Protein Assay Kit	Thermo Fisher Scientific	Cat# 23227
Ceramide/Sphingoid Internal Standard Mixture II	Avanti Polar Lipids	Cat# LM-6002
C16 Ceramide-d7 (d18:1-d7/16:0)	Avanti Polar Lipids	Cat# 860516
C18 Ceramide-d7 (d18:1-d7/18:0)	Avanti Polar Lipids	Cat# 860518
C24 Ceramide-d7 (d18:1-d7/24:0)	Avanti Polar Lipids	Cat# 860524
C24:1 Ceramide-d7 (d18:1-d7/24:1(15Z))	Avanti Polar Lipids	Cat# 860525
Methanol (HPLC grade)	Fisher Scientific	Cat# A456-4
Isopropanol	Fisher Scientific	Cat# A416-4
Ethyl Acetate	Fisher Scientific	Cat# E145-4
Ammonium Formate	Sigma-Aldrich	Cat# 70221
Formic Acid (≥95%)	Sigma-Aldrich	Cat# 94318
Labeled Amino Acids Standards Set A1	Cambridge Isotope Laboratories, Inc	Cat# NSK-A
Metabolomics Amino Acids Mix Standard	Cambridge Isotope Laboratories, Inc	Cat# MSK-A2-1.2
7-methyluric acid-2,4,5,6-13C4,1,3,9-15N3	Sigma-Aldrich	Cat# 705616
Normal chow diet	TEKLAD	Cat# 2916
60% HFD-dox (600 mg/kg doxycycline)	BioServ	Cat# F3282
60% HFD	BioServ	Cat# S1850
Humulin R Insulin	Eli Lilly	Cat# NDC0002-8215-01
Critical commercial assays		
Leptin ELISA Kit	Crystal Chem	Cat# 90080
Adiponectin ELISA Kit	Millipore	Cat# EZMADP-60K
Insulin ELISA Kit	ALPCO	Cat# 80-INSMS-E10
Mouse FGF21 ELISA Kit	Millipore	Cat# EZRMFGF21-26K
IGF1 ELISA Kit	Abcam	Cat# ab100695
NEFA-HR(2) Assay	Wako Diagnostics	Cat# 999-34691
Glucose Assay Kit	Sigma-Aldrich	Cat# GAGO20
Glycerol Reagent	Sigma-Aldrich	Cat# F6428
eBioscience FoxP3 Fix/Perm nuclear staining kit	Thermo Fisher Scientific	Cat# 00-5523-00
Experimental models: Organisms/strains		
Mouse: TRE-FGF21; adiponectin-rtTA	This paper	N/A
Mouse: Adiponectin knockout	Described previously	(Potthoff, M.J. et al.[23])
Mouse: Fgf21 knockout	Described previously	(Nawrocki, A.R et al.[58])

(*Continued on next page*)

Continued		
REAGENT or RESOURCE	SOURCE	IDENTIFIER
Oligonucleotides		
TRE-FGF21 genotyping primers5′-TGCTGCTGGAGGACGGTTAC -3' and 5'-AAGAACAATCAAGGGTCCC -3'	This paper	N/A
Adiponectin-rtTA genotyping primers 5'- TGCAGGTCCTGATTGGATGTG -3' and 5'- TTTCCTTGTCGTCAGGCCTTC -3'.	This paper	N/A
Additional qPCR primers	This paper	See Table S5
Software and algorithms		
Excel	Microsoft	N/A
GraphPad Prism 10	GraphPad	https://www.graphpad.com
FlowJo v10.8.1	BD Biosciences	https://www.flowjo.com
Fiji (ImageJ)	NIH	https://imagej.net
CalR (ANCOVA analysis)	Mina et al.[30]	https://calrapp.org
DAVID 2021	NIH	https://david.ncifcrf.gov
Proteome Discoverer 3.0	Thermo Fisher Scientific	N/A
PrimerBlast	NIH	(https://www.ncbi.nlm.nih.gov/tools/primer-blast/)
Other		
Bayer Contour Glucometer	Bayer	N/A
Chemistry Analyzer Vitros 350	Ortho Clinical Diagnostics	N/A
NuPAGE Bis-Tris XCell SureLock system	Thermo Fisher Scientific	N/A
Keyence BZ-X700 Fluorescence Microscope	Keyence	N/A
Odyssey Infrared Imager	Li-Cor	N/A
EchoMRI-100 Body Composition System	EchoMRI LLC	N/A
TSE Metabolic Chambers	TSE Systems	N/A
QuantStudio 6 Flex System	Thermo Fisher Scientific	N/A
Ascentis Express C8 HPLC column	Supelco,	N/A
Nexera X2 UHPLC + LCMS-8060	Shimadzu	N/A
BD LSR II Flow Cytometer	BD Biosciences	N/A

EXPERIMENTAL MODEL AND STUDY PARTICIPANT DETAILS

Mouse models

All animal experimental protocols were approved by the Institutional Animal Care and Use Committees (IACUCs) of the University of Texas Southwestern (UTSW) Medical Center (protocol #2015–101207). We established doxycycline-inducible, adipocyte-specific FGF21 overexpression by crossing TRE-FGF21 mice with *adiponectin*-rtTA mice. These mice were bred with wild-type C57BL/6J mice, and subsequent litters were tested using PCR genotyping and Sanger sequencing. The genotyping primers TRE-FGF21 were: 5'- TGCTGCTGGAGGACGGTTAC -3' and 5'- AAGAACAATCAAGGGTCCC -3'. The positive transgenic band is 300 bp in size. The genotyping primers for *adiponectin*-rtTA were: 5'- TGCAGGTCCTGATTGGATGTG-3' and 5'- TTTCCTTGTCGTCAG GCCTTC -3'. The positive transgenic band is 300 bp in size. The transgenic mice were crossed with adiponectin knockout mice and *Fgf21* knockout mice that have been previously described.[23,58]

Mice were housed under barrier conditions on a 12-hour light/dark cycle in a temperature-controlled environment (22°C) with free access to food and water and constant veterinary supervision. Water and cages were autoclaved, and cages were changed every other week. The mouse genotype did not cause visible changes in initial weight, overall health, or immune status.

All animals used in this study were littermate-controlled male mice on a pure C57BL/6J background. Only male mice were used as female mice are more resistant to developing obesity and type 2 diabetes. The age and number of the mice used for the experiments are indicated for each experiment in the figure legends. To ensure reproducibility, two separate cohorts of mice were used whenever possible. No inclusion or exclusion criteria were applied, and the experiments were not randomized.

Mice were maintained on a standard rodent chow diet. Where indicated, they were fed a high-fat diet (HFD-dox) or dox-containing HFD-dox (600 mg/kg), (BioServ, Frenchtown, NJ) initiated at 10-12 weeks of age. In all experiments involving HFD-dox feeding, the same diet was provided to all mice, including controls (i.e. mice lacking the inducible transgene *TRE-Fgf21*).

METHOD DETAILS

Body composition analysis

Body fat and lean mass were measured in conscious mice using an EchoMRI-100 system.

Oral glucose tolerance test

Mice were fasted for 4 hours prior to administration of 2.5 g/kg body weight of glucose by gastric gavage. Blood glucose concentrations were measured using Bayer Contour glucometers. During the test, blood was collected from the tail vein at 0, 15, 30, 60, and 120 minutes, and serum was obtained by centrifugation and stored frozen until further measurements.

Insulin tolerance test

Mice were fasted for 4 hours prior to administration of 0.5 U/kg body weight of human insulin (Humulin R) by intraperitoneal injection. Blood glucose concentrations were measured using Bayer Contour glucometers.

Beta-3 adrenergic receptor agonist test

Mice did not fast before the experiment. Tail-vein serum samples were obtained before and 15, 30, 60 and 120 min following intraperitoneal injection of 1 mg kg−1 CL 316,243 (Sigma-Aldrich, St Louis, MO, USA).

Metabolic cages

Transgenic mice and their littermate controls were single housed for a week before and during the metabolic cage studies performed by the UTSW Metabolic Core Facility. Mice were acclimated in the metabolic chambers at room temperature for 5 days before the start of the experiments. The mice were maintained on a 12-hour dark-light cycle at thermoneutral - 30°C, room temperature - 22°C, or cold - 6°C for 24 hours respectively. Metabolic parameters, including oxygen consumption, CO_2 generation, food intake, and locomotor activity, were monitored and recorded continuously using the TSE calorimetric system (TSE Systems). Mice were fed HFD-dox as indicated and water *ad libitum*.

RNA isolation, reverse transcription, and quantitative RT-PCR

RNA was isolated from cells snap-frozen using Trizol, (Invitrogen, Carlsbad, CA, USA). Quality and quantity of the RNA were determined by absorbance at 260/280 nm. cDNA was prepared by reverse transcription using the iScript cDNA Synthesis Kit (Bio-Rad). RT-qPCR was performed using PowerUp SYBR Green Master Mix (Thermo Fisher Scientific) on a QuantStudio 6 Flex system (Thermo Fisher Scientific). Primer sequences are listed in Supplementary Table S5. When validated by the Harvard Primer Bank[81] were unavailable, primers were designed using PrimerBlast (https://www.ncbi.nlm.nih.gov/tools/primer-blast/). Data was analyzed using the threshold cycle (Ct) method with β-actin for normalization. mRNA expression levels were calculated using the ΔΔCt method as described previously.[82]

Blood Parameters

Blood was taken from animals, allowed to clot, and centrifuged for 5 min at 8,000*g* to isolate serum for multiple analyses. Fresh serum was provided for ALTV and AST measurement by Chemistry Analyzer Vitros 350 (Ortho Clinical Diagnostics). Serum samples were frozen for all other measurements. Na+, Mg2+, Ca2+, Lactate, and BUN by Chemistry Analyzer Vitros 350 (Ortho Clinical Diagnostics). Glycerol and glucose levels were determined using a free glycerol reagent and an oxidase–peroxidase assay, respectively (Sigma-Aldrich). TG levels and cholesterol levels were measured using Infinity reagents (Thermo Fisher Scientific, Waltham, MA, USA). FFA levels were measured with a NEFA-HR(2) kit (Wako). Hormones were measured using ELISA kits Leptin (#90080, Crystal Chem) Adiponectin (EZMADP-60K, Invitrogen), Insulin (80-INSMS-E10, APLCO), Mouse FGF21 (Millipore), and Mouse IGF1 ELISA Kit (ab100695, Abcam).

Histology

Tissues were collected, fixed in 10% PBS-buffered formalin up to 2 months at room temperature, and stored in 50% ethanol at room temperature. Following paraffin embedding and sectioning at 5 μm, tissues were stained with H&E.

Stromal vascular fraction isolation and flow cytometry

Adipose tissue was enzymatically digested in HBSS (Life Technologies) with collagenase II (Worthington Biochemicals) with shaking for 45 min at 37°C. The stromal vascular fraction (SVF) cells were collected by at 1500 rpm for 10 min, then treated with ACK lysis buffer (Quality Biological) to remove the red blood cells. After washed and filtered, cells were resuspended in 1 ml of RPMI media (Thermo Fischer Scientific) with 10% FBS and 1% antibiotics (Thermo Fischer Scientific) for counting. For staining, SVF cells were incubated with FcBlock CD16/32 cell antibodies (Thermo Fischer Scientific) for 30 min on the ice, and then cells were stained with live/dead viability dye (Thermo Fischer Scientific) and incubated with surface markers (eBioscience, Biolegend and BD) for 40 min on the ice in the dark. For intracellular staining, Foxp3 was performed using the eBioscience Fix/Perm nuclear staining kit. Flow cytometry was performed on BD LSRII and data was analyzed in FlowJo (v10.8.1). The flow cytometry gating strategy began withlive cells (LD-aqua, Thermo Fischer scientific) selected on a forward scatter area (FSC-A)/side scatter area (SSC-A) plot. Singlets were selected on subsequent forward scatter width (FSC-W) and side scatter width (SSC-W) plots. Unstained cells isolated from wild-type mice were used to determine background fluorescence levels. Cell subpopulations can be distinguished on the basis of different cell surface markers including CD45, CD25,

CD127, St2 and Lin- (CD3, TCRb, CD11b, F4/80, Gr1, FCeRa, Ter119, CD5, CD19, NK1.1) for ILC2, CD45, B220CD21, CD23 for B cells and CD45, B220, CD25, F4/80, CD11c, FoxP3, CD206, CD11b, CD4 for Macrophages. All antibodies were purchased from eBioscience or Biolegend.

Western blotting

For protein lysate, tissue was snap-frozen at −80°C until lysis. Samples were lysed and homogenized in Cell Lysis Buffer (#9803, Cell Signaling) supplemented with Halt Protease and Phosphatase Inhibitors (78442, Thermo Fisher Scientific) for 15min on ice. The supernatant was collected and protein concentrations were determined using the Pierce BCA Protein Assay Kit (Thermo Fisher Scientific). Proteins were resolved in MES or MOPS buffer on Novex 4–12% bis-Tris gels (Thermo Fisher Scientific) and transferred to nitrocellulose membranes using the NuPAGE Bis-Tris XCell SureLock system (Thermo Fisher Scientific). The blots were then blocked with 5% nonfat dry milk for 1 hour at room temperature and then incubated with primary antibodies diluted in 5% BSA blocking buffer overnight at 4°C. The following antibodies were used: anti-β-actin (1:10,000; Sigma Aldrich), anti-FGF21 (1:1,000, BioVendor), anti-AKT (1:2,000) and anti-pAKT (1:2,000), were purchased from Cell Signaling Technology. Primary antibodies were detected using secondary antibodies labeled with infrared dyes emitting at 700 nm or 800 nm (Li-Cor). Secondary antibody staining was performed for 1 hour at room temperature. The blots were then scanned on a LI-COR Odyssey Dlx instrument (Li-Cor Bioscience). The scanned data were analyzed using Fiji software.

Sphingolipid measurements

Ceramides and other sphingolipids were quantified by liquid chromatography-electrospray ionization–tandem mass spectrometry.[50] Tissue samples (50 mg) and serum samples (30 μL) were homogenized in 4.0 mL organic extraction solvent (isopropanol: ethyl acetate, 15:85; v:v). Immediately afterward, 20 μL internal standard solution was added (Ceramide/Sphingoid Internal Standard Mixture II at a 10 fold dilution in methanol combined with a mixture of C16 Ceramide-d7 (d18:1-d7/16:0), C18 Ceramide-d7 (d18:1-d7/18:0), C24 Ceramide-d7 (d18:1-d7/24:0), and C24:1 Ceramide-d7 (d18:1-d7/24:1(15Z)) at a concentration of 2.4 μM, Avanti Polar Lipids, Alabaster, AL). The mixture was vortexed and 3.0 mL of HPLC water was added. Two-phase liquid extraction was performed, the supernatant was transferred to a new tube, and the aqueous phase was re-extracted. Supernatants were combined and evaporated under nitrogen. The dried residue was reconstituted in 200 μL of MeOH. Sphingolipid profiling was conducted by liquid chromatography-electrospray ionization-tandem mass spectrometry (LC-MS/MS), using a Nexera X2 UHPLC coupled to an LCMS-8060 (Shimadzu Scientific Instruments, Columbia, MD, USA). 3 μL and 1 μL of sample was injected for the analysis of sphingoid bases and ceramides, and sphingomyelins, respectively and the autosampler was kept at 9 °C during the duration of the batch analysis. Lipid separation was achieved by reverse-phase liquid chromatography on a 2.1 × 150 mm, 2.7 μm Ascentis Express C8 HPLC column (Supelco, Bellefonte, PA) using a gradient elution with H2O 5 mM ammonium formate 0.8% formic acid (v/v) and MeOH 5 mM ammonium formate 0.8% formic acid (v/v).

Amino acid measurements

Amino acid levels were analyzed as previously described.[83] Liver tissue samples were homogenized 5% solution of trichloroacetic acid (1:10 tissue-to-solvent-ratio (w/v)). Adipose tissue samples were homogenized 5% solution of trichloroacetic acid (1:5 tissue-to-solvent-ratio (w/v)). 10 μL of serum samples and tissue homogenates were added to 150 μL of MeOH, immediately after wards 20 μL was added and 20 μL of internal standard cocktail mixture. The internal standard cocktail mixture was prepared by mixing 100 μL of Labeled Amino Acids Standards Set A1 (Cambridge Isotope Laboratories, Inc., Tewksbury, MA), 50 μL of Metabolomics Amino Acids Mix Standard (Cambridge Isotope Laboratories, Inc.), 1.0 mL of an aqueous solution of 7-methyluric acid-2,4,5,6-13C4,1,3,9-15N3 (99% atom %13C, 98 atom % 15N, 97% (CP); Sigma-Aldrich, St Louis, MO) at a 529 μM concentration, and 3.15 mL of HPLC water. The samples were vortexed for 30 seconds and centrifuged in a benchtop micro centrifuge at 17,000 g at 4 °C for 10 minutes. Supernatant was then transferred to a low absorption polypropylene autosampler vials. Samples were analyzed on a Nexera X2 UHPLC system coupled to an LCMS-8060 triple quadrupole mass spectrometer (Shimadzu Scientific Instruments). 2 μL was injected onto the analytical system and the autosampler was kept at 4 °C during the duration of the batch analysis. Free amino acids were analyzed using the mass spectrometry parameters and chromatographic conditions described in the Shimadzu LC/MS/MS Method Package for Cell Culture Profiling.

Tandem mass tag mass spectrometry

For protein lysate, tissue was snap-frozen at −80°C until lysis. Samples were lysed and homogenized in Cell Lysis Buffer (#9803, Cell Signaling) with Halt Protease and Phosphatase Inhibitors (78442, Thermo Fisher Scientific) for 15min on ice. Lysate was centrifuged at 15000xg for 15min at 4°C. The supernatant was collected and submitted to UTSW Proteomics Core for TMT-16plex. Data was analyzed using Proteome Discoverer 3.0 and was searched using the human protein database from UniProt.

QUANTIFICATION AND STATISTICAL ANALYSIS

No statistical method was used to predetermine the sample size. The experiments were not performed blinded. Data are displayed as mean ± standard error of the mean (SEM). All statistical analyses were performed using Prism software (GraphPad). A Student's t test was used to compare two independent groups. For mouse experiments, each biological replicate corresponds to a separate mouse.

Differences between multiple conditions and two groups over time were evaluated using two-way ANOVA with Geisser-Greenhouse and Tukey's post-doc test for multiple comparisons. GraphPad Prism 10.0 (San Diego, CA, USA) was used to calculate the area under the curve (AUC) of glucose compared between groups using an unpaired t-test. Gene ontology (GO) enrichment analyses were conducted with DAVID 2021 (https://david.ncifcrf.gov/). The significant cut-off criterion was FDR < 0.05 (*p*-value adjusted for multiple tests by the Benjamini-Hochberg procedure).